



HAL
open science

Use of Electrical Resistivity Tomography measurements for investigation of different grouting materials for very shallow geothermal applications within varying seasonal conditions; applied on a geothermal Earth-Air Heat Exchanger system.

Hans Schwartz, Jian Lin, David Bertermann

► To cite this version:

Hans Schwartz, Jian Lin, David Bertermann. Use of Electrical Resistivity Tomography measurements for investigation of different grouting materials for very shallow geothermal applications within varying seasonal conditions; applied on a geothermal Earth-Air Heat Exchanger system.. *Renewable Energy*, 2024, in press, 10.1016/j.renene.2024.120664 . hal-04589924v1

HAL Id: hal-04589924

<https://hal.science/hal-04589924v1>

Submitted on 27 May 2024 (v1), last revised 5 Jul 2024 (v2)

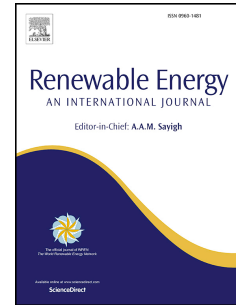
HAL is a multi-disciplinary open access archive for the deposit and dissemination of scientific research documents, whether they are published or not. The documents may come from teaching and research institutions in France or abroad, or from public or private research centers.

L'archive ouverte pluridisciplinaire **HAL**, est destinée au dépôt et à la diffusion de documents scientifiques de niveau recherche, publiés ou non, émanant des établissements d'enseignement et de recherche français ou étrangers, des laboratoires publics ou privés.

Journal Pre-proof

Use of Electrical Resistivity Tomography measurements for investigation of different grouting materials for very shallow geothermal applications within varying seasonal conditions; applied on a geothermal Earth-Air Heat Exchanger system.

Schwarz Hans, Lin Jian, Bertermann David



PII: S0960-1481(24)00732-8

DOI: <https://doi.org/10.1016/j.renene.2024.120664>

Reference: RENE 120664

To appear in: *Renewable Energy*

Received Date: 4 June 2023

Revised Date: 10 May 2024

Accepted Date: 13 May 2024

Please cite this article as: Schwarz H, Lin J, Bertermann D, Use of Electrical Resistivity Tomography measurements for investigation of different grouting materials for very shallow geothermal applications within varying seasonal conditions; applied on a geothermal Earth-Air Heat Exchanger system., *Renewable Energy*, <https://doi.org/10.1016/j.renene.2024.120664>.

This is a PDF file of an article that has undergone enhancements after acceptance, such as the addition of a cover page and metadata, and formatting for readability, but it is not yet the definitive version of record. This version will undergo additional copyediting, typesetting and review before it is published in its final form, but we are providing this version to give early visibility of the article. Please note that, during the production process, errors may be discovered which could affect the content, and all legal disclaimers that apply to the journal pertain.

© 2024 Published by Elsevier Ltd.

Title:

Use of Electrical Resistivity Tomography measurements for investigation of different grouting materials for very shallow geothermal applications within varying seasonal conditions; applied on a geothermal Earth-Air Heat Exchanger system.

Authors:

Schwarz, Hans^a, Lin, Jian^b, Bertermann, David^a

Affiliations:

^aGeoZentrum Nordbayern, Department Geographie und Geowissenschaften, Friedrich-Alexander-Universität Erlangen-Nürnberg, Schlossgarten 5, 91054 Erlangen, Germany

^bICUBE(UMR7357), IUT Robert Schuman, University of Strasbourg, 67400 Illkirch-Graffenstaden, France

Correspondence: hans.schwarz@fau.de

Authors contact: hans.schwarz@fau.de, jlin@unistra.fr, david.bertermann@fau.de

1 Title:

2 Use of Electrical Resistivity Tomography measurements for investigation of different grouting
3 materials for very shallow geothermal applications within varying seasonal conditions; applied on a
4 geothermal Earth-Air Heat Exchanger system.

5 Authors:

6 Schwarz, Hans^a, Lin, Jian^b, Bertermann, David^a

7
8
9 ^aGeoZentrum Nordbayern, Department Geographie und Geowissenschaften, Friedrich-Alexander-
10 Universität Erlangen-Nürnberg, Schlossgarten 5, 91054 Erlangen, Germany

11 ^bICUBE(UMR7357), IUT Robert Schuman, University of Strasbourg, 67400 Illkirch-
12 Graffenstaden, France

13 Correspondence: hans.schwarz@fau.de
14
15

16 Abstract:

17
18 To achieve the current climate targets, heat pump systems like very shallow geothermal applications
19 are gaining ground. However, the dimensioning of these ground coupled systems is soil-dependent
20 and thus subject to significant differences in efficiency. Furthermore, the thermal properties of the
21 grouting materials are essential for heat transfer in the direct vicinity of the geothermal application.
22 To provide a non-invasive assessment of relevant soil and grouting characteristics, electrical
23 resistivity tomography (ERT) measurements were performed.

24 In this case, the surrounding of an Earth Air-Heat Exchanger – system (EAHE) with different grouting
25 materials (fine sand and fine sand with bentonite) was investigated. For investigation the electrical
26 resistivity (ER) of initial and modified soil conditions were measured regarding soil texture and
27 moisture content. Thereby, the different grouting materials are clearly identified. Thus, based on the
28 ERT measurements, a characterisation of key soil and grouting material properties for applications
29 focusing on heat transfer in soil has been carried out.

30 Furthermore, the depth of soil disturbance due to the EAHE installation could have been traced.

31 Due to a monitoring over different season (February and May) changes in raw ER data could have
32 been ascribed to temperature changes.
33

34 Keywords: electrical resistivity tomography, soil properties, earth air-heat exchanger, very shallow
35 geothermal, grouting material, seasonal impact
36
37

38 -1. Introduction

39
40 Renewable energies are indispensable for meeting climate targets and for increasing independence
41 from the import of fossil fuels. For meeting the demand of thermal and cooling energy, very shallow
42 geothermal systems can play an important role.

43 One general difficulty of very shallow geothermal systems is the determination of an accurate
44 dimension to meet particular energy demands. For installations of vertical borehole heat exchangers
45 Thermal Response Tests (TRT) can be performed [1-3] even though neighbourhood effects may occur
46 [4, 5], but for horizontal very shallow systems such a standardised process is not yet established. This
47 is also due to a bright variety of very shallow geothermal systems [6] and due to the easy adaptability
48 of the systems configuration, which also shows a performance influence [7]. Regarding very shallow
49 geothermal applications, to make economies usually an appropriate soil assessment for a proper and
50 soil depending installation is not commissioned. In addition, the grouting material in the immediate
51 vicinity of the ground source heat exchanger (GSHE) also has a major influence on the efficiency of

52 the system [8-12]. However, there are no specific guidelines with focus on grouting for horizontal
53 geothermal installations either [13]. And in most cases, this involves the use of vertical probe systems.
54 Consequently, many systems are dimensioned inadequate. For safety reasons, very shallow
55 geothermal installations are dimensioned mostly too big, by just using a rule of thumb. In cases of
56 space scarcity, this can be an evitable knock-out criterion for these very shallow geothermal systems.
57 However, in order to match the dimensions of these geothermal systems according to the geothermal
58 potential of the ground environment, the soil properties and the grouting characteristics with regard
59 to heat transport must be known.

60
61 For convenient recommendations on the feasibility of very shallow geothermal installations
62 information of the soil properties thermal conductivity, water content, bulk density and soil type are
63 needed [8, 10, 14, 15]. Such information could be delivered by geothermal potential maps [6, 16].
64 But these potential maps cannot substitute detailed on-site investigations.

65
66 By applying Electrical Resistivity Tomography (ERT) measurements within this study a non-invasive
67 investigation method is tested for examinations on the basic parameters that are decisive for the
68 thermal properties. In comparison to selective drilling points, by measuring ERT sections, a large
69 area can be covered for a continuous soil screening. Formerly self-potential measurements were
70 performed to examine deeper geothermal systems [17, 18]. Generally, ERT measurements are
71 influenced by several physico-chemical soil properties [19, 20]. Particularly, ER is very sensitive to
72 water content of soil [20-25], whereby the groundwater level can be additionally detected if present.
73 Another influencing parameters are soil texture and bulk density, and even if they are not as decisive
74 as water content these parameters can conversely be derived from ER [26]. Moreover, temperature is
75 influencing the ER measurement results [27-30], which is analysed in this study and reflected in the
76 temperature correction models [19, 31]. Since the same soil physical properties affect the electrical
77 resistivity as well as the thermal conductivity of soil [32-35], ERT data can be used to derive soil
78 thermal parameters [36-40] as key parameters for defining a geothermal potential.

79
80 However, until now for investigations of the ground thermal properties around very shallow
81 geothermal systems, ERT measurements have been used rarely [28, 41-44]. Just a few investigations
82 regarding very shallow geothermal systems are focusing on heat propagation [45-47]. And none of
83 these investigations were applied to an earth air-heat exchanger – system (EAHE), which is an air
84 conveying GSHE buried in very shallow depth like other very shallow geothermal applications [48-
85 54]. As it applies for all GSHE installations, the ground is utilized as heat sink or heat source. Hence,
86 its energy performance depends on the physical-thermal properties of the surrounding material [8, 9,
87 55].

88
89 Thus, within this study the soil and grouting material surrounding of a EAHE as a GSHE installation
90 was investigated with ERT measurements. The objective was on the one hand to categorise the soil
91 texture and the grouting material in terms of ER and on the other hand to evaluate the effect of variable
92 grouting materials, seasonal variation of soil temperature and the running of the EAHE on the
93 measured ER values. At the same time the investigated effect of a changing soil temperature assesses
94 the robustness of the ERT measurement. To do so the ERT measurements were carried out at spring
95 and winter seasons, and at each time with running and shutdown of the EAHE system. The
96 measurements were carried out on a EAHE test site in Strasbourg France, where different grouting
97 materials are installed. The fact that the different grouting materials at the site have an influence on
98 the energy performance of the EAHE system has already been investigated [8, 9]. Lin et al. [55] have
99 already studied the impact of soil moisture on the energy performance of this system and also the
100 influence of rainfall events [56]. So, the effect of different parameters on the energy performance of
101 the very shallow geothermal system was already investigated and the main task in this study was to
102 measure these influencing parameters in the vicinity of a very shallow geothermal installation with a

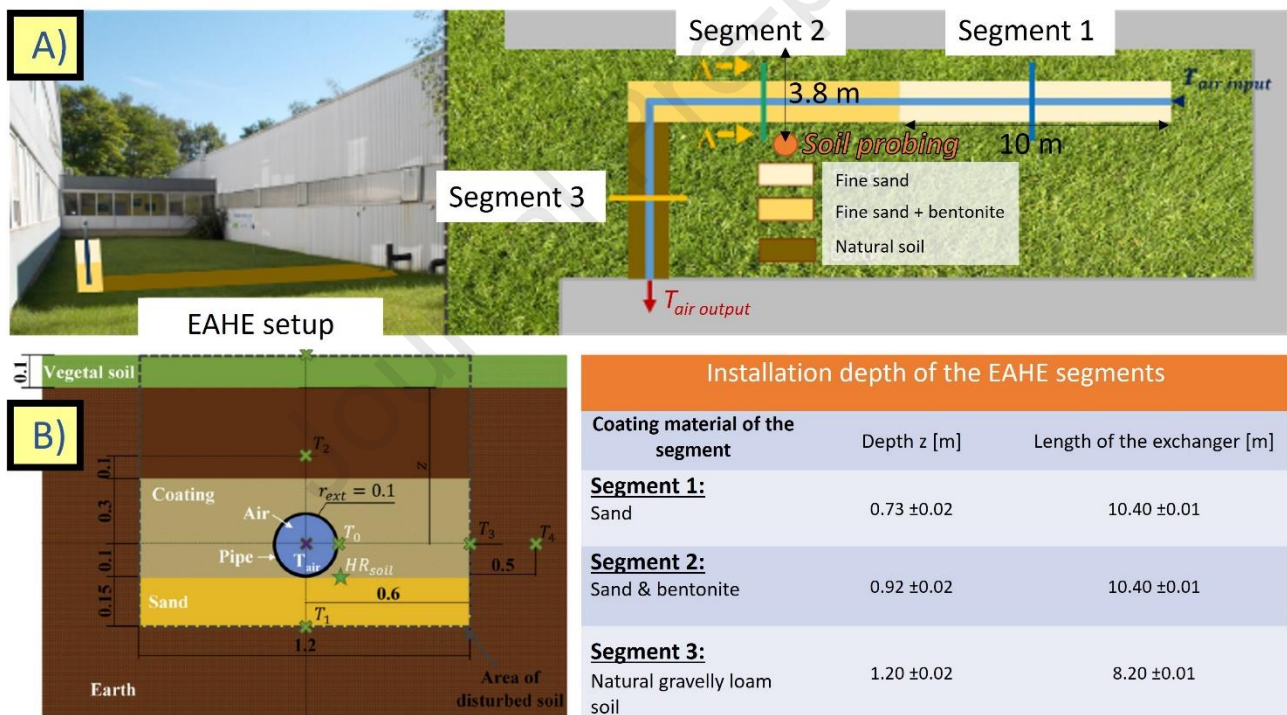
103 preferably fast and non-invasive method. At the same time, soil temperature is shown as an interfering
 104 factor that users should definitely take into account when interpreting ER.
 105

106 Such an investigation method should enable recommendations on the determining soil factors for an
 107 estimation of feasibility and the dimensioning of very shallow geothermal systems. The advantage of
 108 this method is the performance directly on-site in a fast and cost-efficient way. Due to the fact that,
 109 the non-invasive ERT measurements can also be applied after the installation works, also an
 110 inspection of the added grouting material is possible.
 111

112 -2. Research methodology

113 2.1 Presentation of the geothermal site in Strasbourg.

114
 115 The EAHE site of this study is located in France at the Civil Engineering department of University
 116 of Strasbourg. The EAHE is divided into three segments that are associated with a different groutings
 117 as coating soil material: (1) fine sand; (2) a mix of fine sand and bentonite (10 %), (3) and natural soil
 118 backfill composed of gravel-clay mixture, respectively (Figure 1). Within the second segment, the
 119 same fine sand has been used in the first segment of the EAHE as the coating soil. The sand used
 120 within the sand coating segment is also implemented as bedding material within all segments.
 121



122

Figure 1: Test site with the EAHE installation at the Civil Engineering department of University of Strasbourg. A) View over the test site on the left and an aerial perspective on the right and B) slice of the installed EAHE system with the dimensions of the pipe, the coating material and the sand bedding with a table of the installation depth of each segment (adjusted from [8])

123

124 The heat exchanger surrounding corresponds to the rectangular excavation form, which is 1.2 m wide
 125 and 0.55 m high, where the lower 15 cm are filled with the bedding sand and the upper 40 cm with
 126 the coating material (Figure 1 **Error! Reference source not found.**). The heat exchanger pipe has a
 127 regular slope of 2%, which is imposed to avoid the stagnation of condensation water. For that reason,
 128 installation depth is increasing by a few decimetres along the system (Figure 1). Within the sand

129 segment the pipe coating starts at an average of 0.53 m below surface. The coating starts at a depth
 130 of 0.72 m (average) regarding the second segment and at 1.00 m depth (average) within segment 3.

131
 132

133 2.2 Information of soil texture

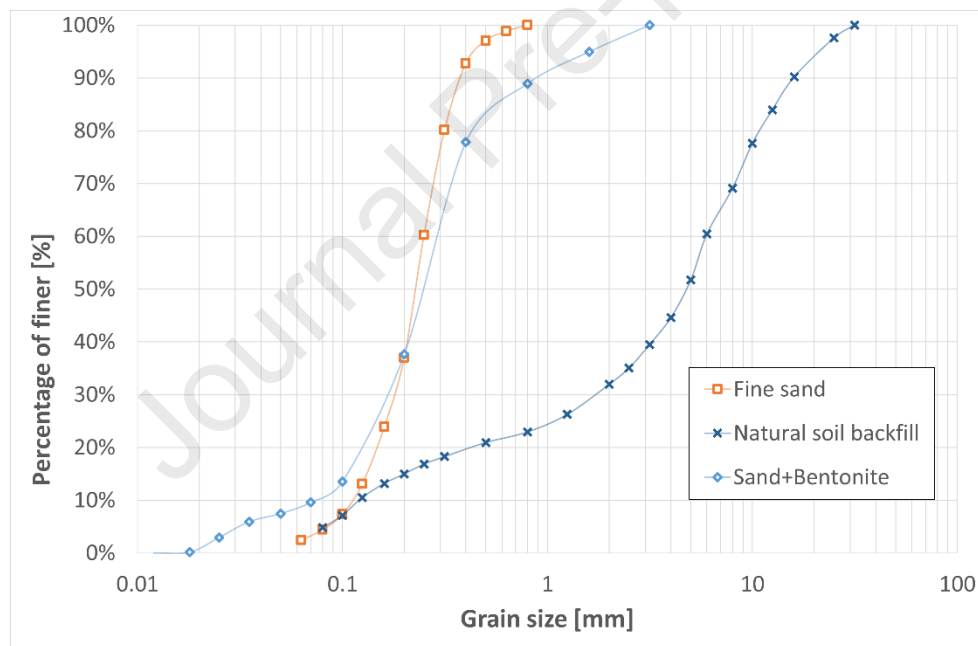
134

135 In order to analyse the surrounding soil layers around the GSHE, within this study a soil probing was
 136 carried out in the EAHE area of the second segment while the installation works took place. In the
 137 investigated spot the sand-bentonite coating starts at 67 cm depth, which is due to the more anterior
 138 position less than the average of 72 cm for this segment. Within a depth from 93 cm until 127 cm the
 139 sand bedding was incorporated, below which the natural soil is following. It has to be considered,
 140 that this ascertained installation depth of the sand beddings lower bound is significantly deeper than
 141 in theory. This shows possible differences towards the installation scheme of [8] and potential thicker
 142 bedding sand layers.

143

144 A granulometric analysis was performed to obtain the grain size distribution of the different
 145 implemented soil types as grouting materials that are already investigated with regard to their thermal
 146 properties [8, 55]. Sieving of dry soil sample was carried out for each soil type. An additional
 147 sedimentation measurement was performed for the mix of sand and bentonite due to the importance
 148 of its content of fine particles (grain size < 0.1 mm) (Figure 2).

149



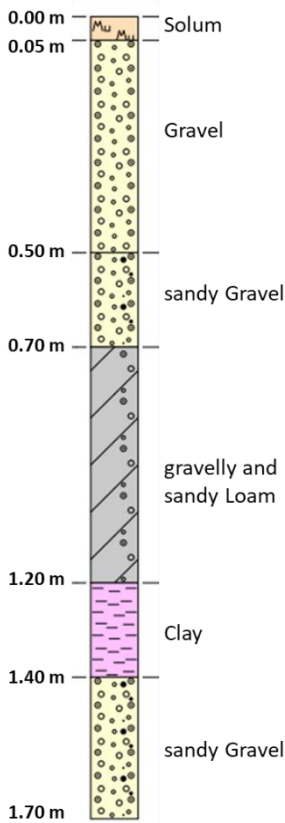
150

151 *Figure 2: Granulometric analysis of the different used soil materials*

152

153 Beside the soil probing in the course of the EAHE system installation an additional soil probing in
 154 the area, of initial field conditions (area of ERT measurement section 2) was carried out. This probing
 155 was performed with a drill hammer.

156 The soil profile of initial field was recorded until a depth of 1.7 m, because with the used probing
 157 application a deeper penetration was not possible due to the gravel (Figure 3). The topsoil is just 0.05
 158 m deep followed by a soil layer composed of gravel-clay until 0.7 m depth. Subjacent, there is loamy
 159 soil down to 1.2 m with some coarse gravel fragments, which also might be due to a collapse of the
 160 borehole. From 1.2 m until 1.4 m a pure clay is following. The lowest recorded layer was gravel with
 161 sand that reached up to 1.7 m.



162

Figure 3: Soil profile of the initial field conditions determined by a drill hammer investigation within the area of ERT measurement section 2.

163

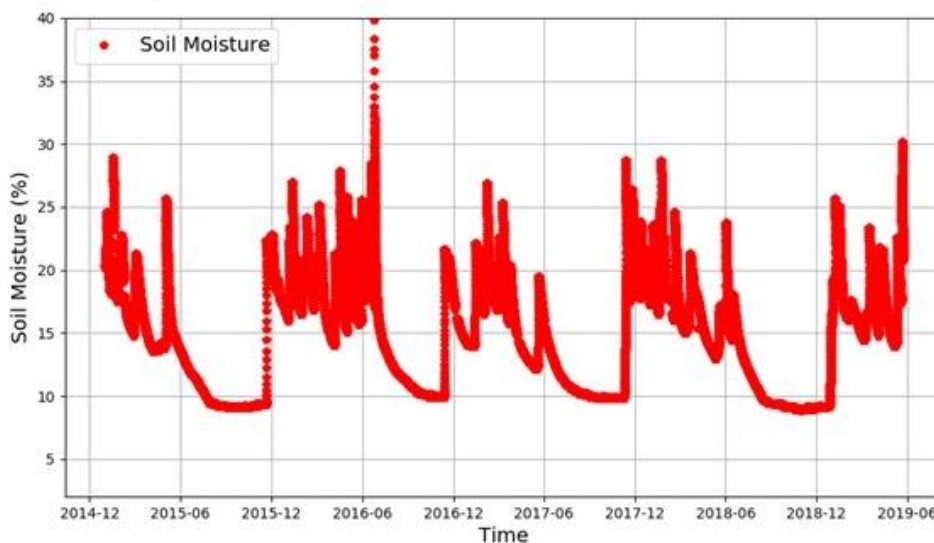
164 2.3 Seasonal soil conditions

165

166 To get an indication of a seasonal impact within the relevant depth of very shallow geothermal
 167 installations by measuring the ER, the ERT measurements were carried out in May 2019 and February
 168 2020. The soil parameters that are seasonal are soil moisture content and soil temperature.

169

170 2.3.1 Soil moisture seasonal variation



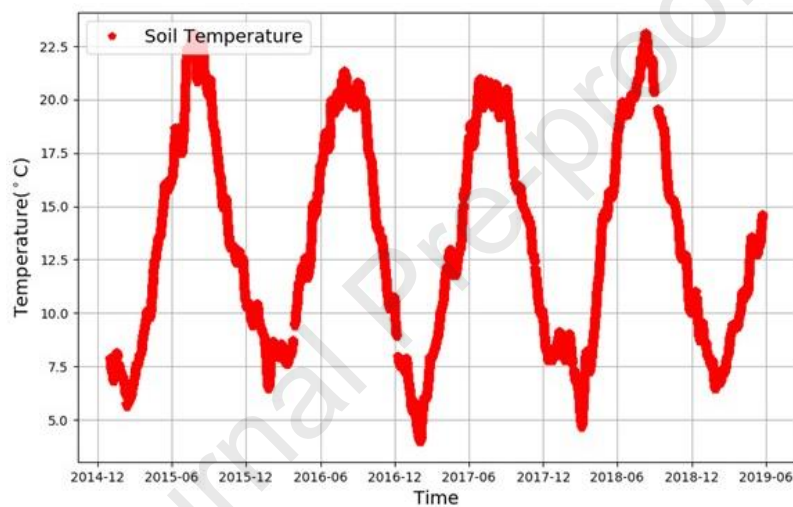
171

Figure 4: Soil moisture [in Wt-%] trend over several years within the fine sand segment of the EAHE installation (segment 1).

172 To describe this seasonal variation of soil moisture this parameter was monitored over several years
173 (Figure 4). Over this period soil moisture was volatile around 15 Wt-% until 25 Wt-% in winter and
174 spring, depending on precipitation quantities, and dried down to 9 to 10 Wt-% at the end of summer.
175 This displays the situation in the installation depth of the heat exchanger. Within deeper or more
176 shallow soil layers, this seasonal influence has a correspondingly greater or lesser effect.
177 In order to avoid great soil moisture difference at the test site for a focus on temperature variability,
178 the summer period was avoided and the two chosen test seasons are winter and spring.
179

180 2.3.2 Soil temperature seasonal variations

181
182 In addition to soil moisture, soil temperature is the simplest and most direct indicator of seasonal
183 changes. This parameter was also monitored in the installation depth of the heat exchanger. In case
184 of this parameter, no variations occurred between the different segments. As shown in Figure 5 on
185 the dates in early February, soil temperatures were around 8.0 °C. The soil temperatures in May were
186 then already significantly higher at 13.0 °C.
187



188

189 *Figure 5: soil temperature trend over several years at the depth of the EAHE installation.*

189

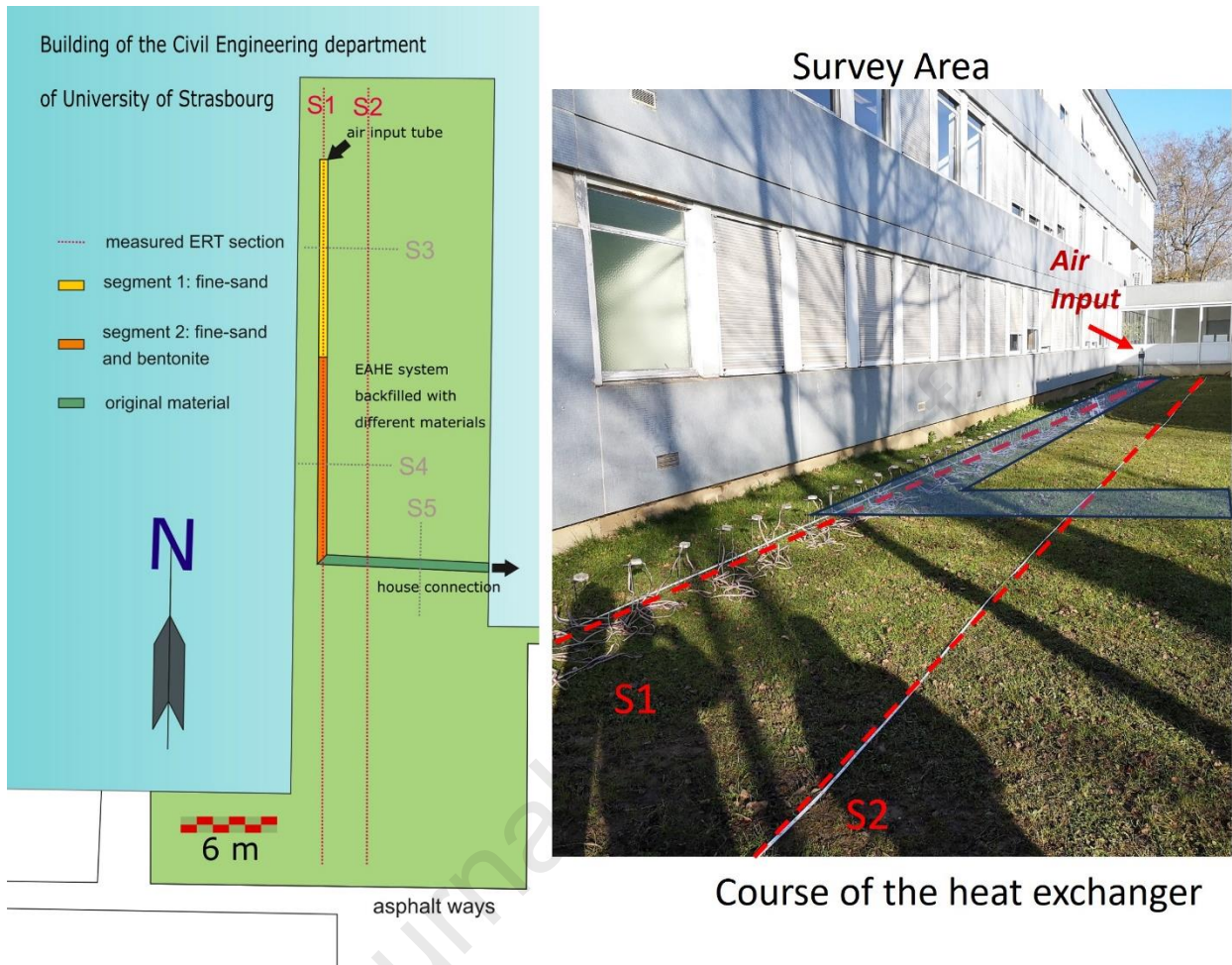
190

191 2.4 ERT measurement and data process

192

193 2.4.1 ERT measurements

194



195

Figure 6: Scheme (left) and picture (right) of the survey area at the Civil Engineering department of University of Strasbourg. Position of the electrical resistivity (ERT) measurements S1 and S2 on the horizontal heat exchanger (EAHE). Measurement application for the measurement of S2.

196

197 Within this survey the ERT sections were measured with the ‘4point light’ resistivity meter of LGM—
 198 Lippmann Geophysical Equipment and the GeoTest software developed by Geophysics—Dr. Rauen
 199 within two field campaigns in May 2019 and February 2020. Each ERT section (Figure 6 **Error! Reference source not found.**)
 200 **Reference source not found.**) was measured twice per field campaign: the first time was carried out
 201 on the first day while the EAHE system was still running and the second time was performed the day
 202 after while the heat exchanger system was shut down. Since the system was shut down in the evening
 203 after the first measurements, the soil temperatures around the EAHE system had a recovery time of
 204 at least 15 h.

205

206 By using the ‘4point light’ device, the ER or rather the electrical conductivity of the underground was
 207 determined in form of 2D-ERT profiles. As shown in Figure 6 **Error! Reference source not found.**,
 208 two sections (S1+S2) were measured with 80 electrodes and a spacing of 50 cm each. S1 was
 209 performed upon the heat exchanger in a distance of 1,2 m to the building. S2 serves as a reference on
 210 the original soil composition and was also measured parallel to the building with a distance of 3.75 m.
 211 S2 keeps a parallel distance of 2.55 m with S1. The heat exchanger area underneath S1 starts between
 212 electrode 8 and 9 (around the 4th meter) and turns to the hall of the Civil Engineering department after
 213 the second segment between electrode 51 and 52 (around the 25th meter).

214

215 Furthermore, three short sections S3, S4 and S5 were measured in a width of 6.0 m with a spacing
216 20 cm. The aim of measurements of these 3 short sections is to reveal the different EAHE grouting
217 materials. However, due to the proximity of the heat exchanger to the building, the investigated zone
218 (surrounding soil of the heat exchanger) could not be recorded in its entirety. Moreover, the
219 penetration depth of these short sections was not sufficient for a proper identification of the focused
220 layers at the EAHE installation depth. Taking this into account, these short sections were not used for
221 further investigations of this study.

222

223 The measurements were carried out using the Wenner array [57-59] because it is less sensitive to
224 noise, especially near buildings, and it enables reasonable results regarding horizontal soil layers. The
225 set frequency was 4.16 Hz.

226

227 2.4.2 ERT data processing

228

229 In the aftermath of the measurements the raw resistivity data was processed to determine the effective
230 ER. Therefore, data inversion was performed with the Res2Dinv software by Aarhus GeoSoftware
231 previously Geotomosoft.

232 In order to have a cohesion in the evaluation of soil ER values, some corrupted datapoints were
233 exterminated before the inversion process. This step concerns especially the S1 measurements which
234 are affected by presence of the vertical air input tube of the EAHE system at the beginning position
235 of the first segment.

236

237 A refined model with a grid width = $0.5 \cdot$ electrode spacing was used for inversion process. Moreover,
238 a robust inversion method with the complete Gauss-Krüger computation was carried out for several
239 iterations. Regarding the data investigation of this study the 5th iteration of each inversion process
240 was used. For graphical depiction of the ERT results the same contour intervals were applied.

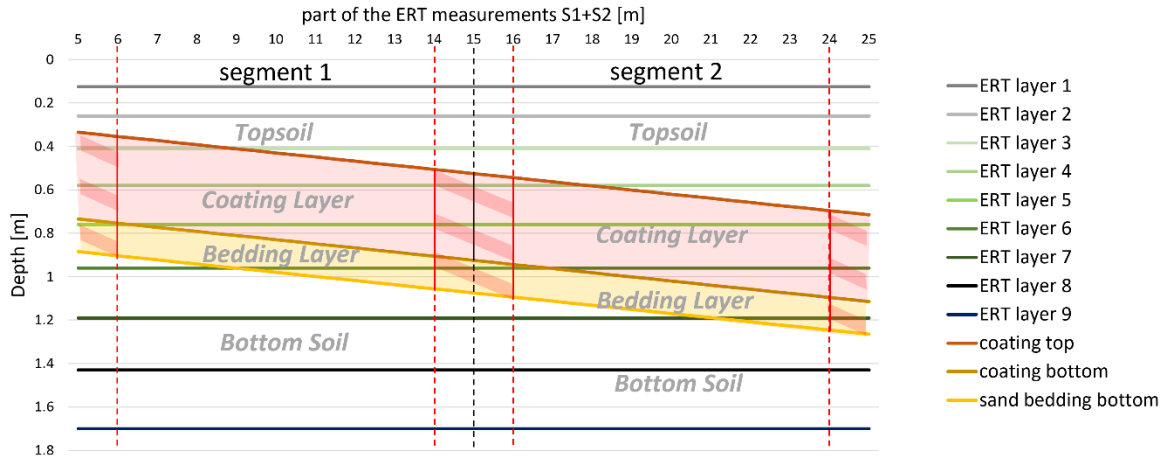
241

242 2.4.3 ERT data analysis

243

244 For a further detailed investigation of the ER values of both sections S1 and S2, the inversion data of
245 the 5th iteration was exported to an Excel-format file. Within this analysis, ERT data of 9 depth layers
246 were used. With the aim to evaluate the ER values with the information of different soil textures,
247 these 9 depth layers were superimposed by different soil domains of the EAHE site as shown in Figure
248 7. 4 types of soil and grouting domains were considered in the analysis: Topsoil, Coating Layer,
249 Bedding Layer, and Bottom Soil, which is the in-site soil beneath the installation.

250



251

Figure 7: Depths of the measured ERT data layers, that are used for further analysis and the depths of the EAHE installation over the distance of of segment 1 and segment 2 taking into account the omitted border areas. The cutting lines “coating top”, “coating bottom”, and “sand bedding bottom” define the exact affiliation of the data points on each ERT layer.

252

253 Thereafter, ER values were classified by soil domains and analysed. This classification was applied
 254 to data of S1 section but also to that of reference section S2 for comparison purpose. The average
 255 value of ER in each soil domain was used in further comparison analysis. To avoid edge effect, ER
 256 values near the transient area of two different segments were not included in the calculation of the
 257 average values (Figure 7).

258

259 To improve comparability of ER values the raw resistivity values are corrected by temperature (T)
 260 according to [19, 31]. Therefore, the reciprocal value of ER, the EC values (σ_T) are processed as the
 261 following equations (1+2).

$$\Sigma_{25} = f_T \cdot \sigma_T \quad (1)$$

$$f_T = 0.4470 + 1.4034 \cdot e^{-T/26.815} \quad (2)$$

262 In the case of this study, the used temperature values are $T = 8 \text{ }^\circ\text{C}$ for February and $T = 13 \text{ }^\circ\text{C}$ for
 263 May, since these temperatures were monitored in the depth of the heat exchanger.

264 However, it has to be considered that the used temperatures for correction refer to soil temperature in
 265 installation depth of the EAHE system. A gradual temperature profile was not taken into account.

266

267 -3. Experimental Results

268

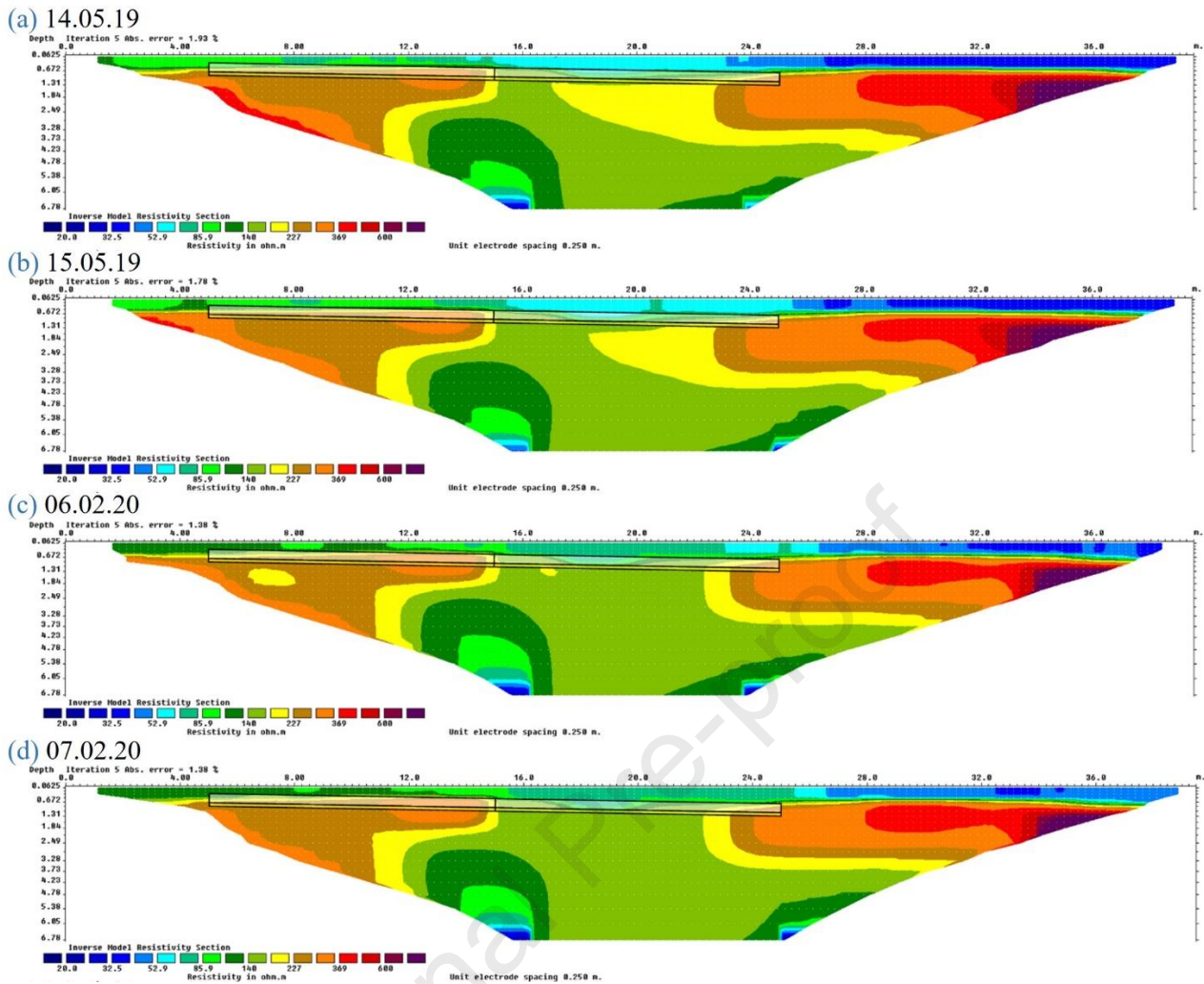
269 3.1 Results of ERT measurement

270

271 To show the distribution of the ER [$\Omega \cdot \text{m}$] below the subsurface, the inverted results of the ERT
 272 measurements, performed within different seasons upon the EAHE system (Figure 8), and of the
 273 reference measurement (Figure 9) are displayed. By applying an ERT section length of 39.5 m a
 274 maximum penetration depth of around 6.8 m was achieved.

275 The left side of the depicted profiles is determined by the placement of the first electrode and the
 276 measurement device, which corresponds to the northern end of the sections. Contour intervals for ER
 277 are determined logarithmic with a start value of 20 $\Omega \cdot \text{m}$ and a multiplier of 1.275.

278



279

Figure 8: ER distribution of the measured section S1 upon the EAHE system, while the heat exchanger system was running (14.05.2019 (a); 06.02.2020 (c)) and after shutting down the heat exchanger system (15.05.2019 (b); 07.02.2020 (d)). The ER values are according to the 5th iteration of the inversion process. Both grouting segments (left: fine sand; in the middle of the section: fine sand and bentonite) with the underlying sand bedding are delineated by black lines.

280

281

282

283

284

285

286

287

288

289

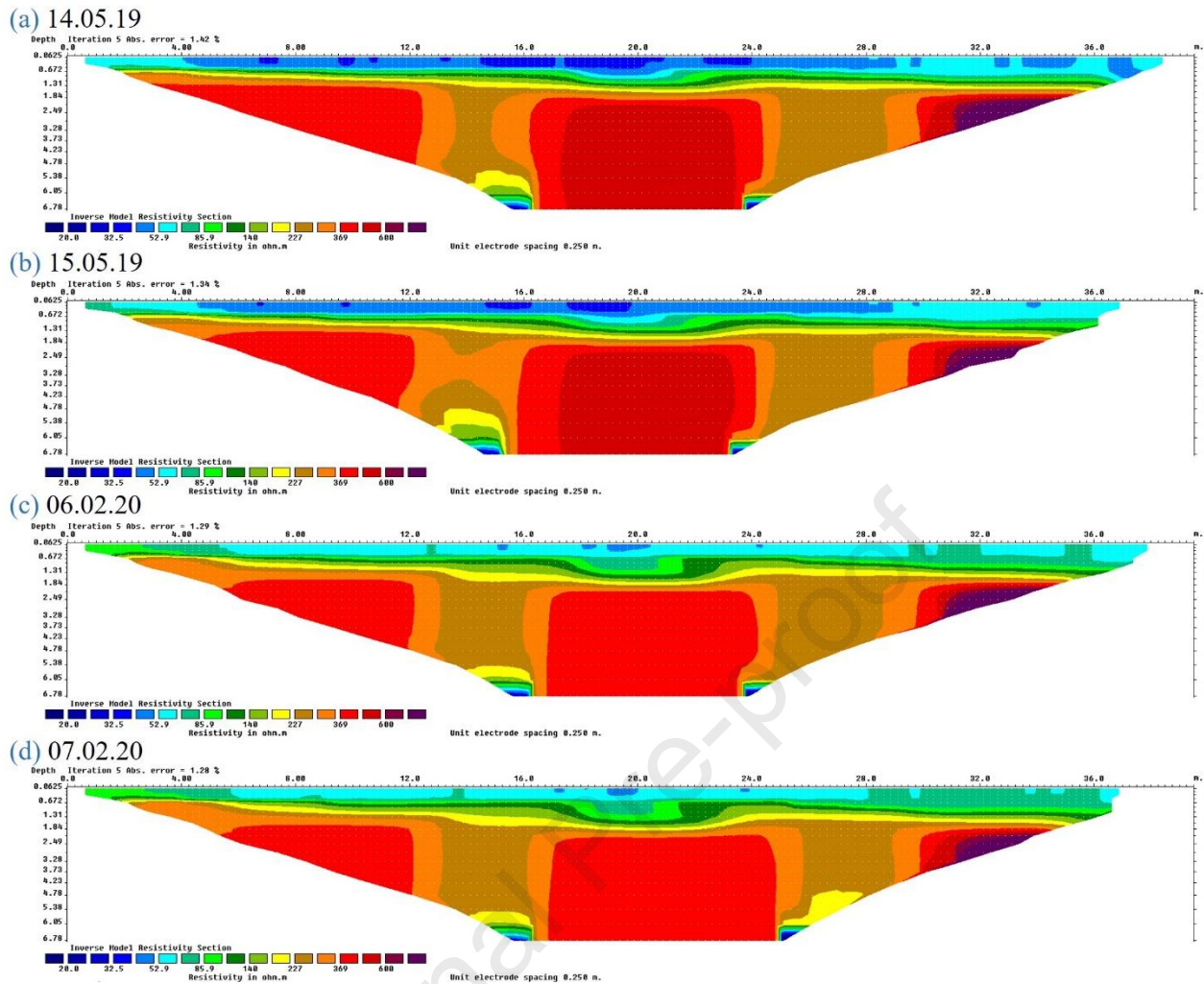
290

291

292

Regarding S1 (Figure 8), there are specific ER values on top of the profile that vary from 40 Ω *m to above 100 Ω *m. Below 0.5 m depth ER rises in parts clearly above 140 Ω *m. This depth of around 0.5-0.7 m corresponds also to the top of the grouted segments. Within the depth of the EAHE installation, the ER shows distinct variabilities between 140 Ω *m and 350 Ω *m.

To verify the influence of the EAHE installation, the results were compared to the undisturbed conditions measured within S2 (Figure 9). The ER values of the topsoil of S2 are around 40-80 Ω *m and with that they are in a similar range compared to the topsoil resistivities of S1. Moreover, the ER within this topsoil in S2 is more evenly distributed than that in S1. This more homogeneously distributed and less variation ER values are also observed for the soil layers below the topsoil. Overall, the highest ER values within greater depths are around 300-500 Ω *m.



293

Figure 9: ER distribution of the measured section S2 as reference while the heat exchanger system underneath S1 was running (14.05.2019 (a); 06.02.2020 (c)) and after shutting down the heat exchanger system (15.05.2019 (b); 07.02.2020 (d)). The ER values are according to the 5th iteration of the inversion process.

294

295 3.2 Comparison of initial field section S2 and the EAHE installation section S1

296

297 To enable an accurate comparison between the initial field section S2 and the EAHE installation
 298 section S1 as well as between both domains of grouting materials (segment 1 and segment 2), the ER
 299 values at different positions were averaged regarding the different domains as described in Figure 7
 300 and corrected for temperature by using equations (1) and (2).

301 It should be considered that the two segment zones are also applied at the reference section S2 for the
 302 purpose of comparison with S1. There is not a real soil difference between these two segments at
 303 section S2.

304 Table 1 shows average ER values at the two EAHE grouting segments for section S1 and section S2.
 305 Each average value is calculated from the 4 ER values derived from the 4 measurements performed
 306 on the same zone (2 at May and 2 at February).

307

Table 1 : Temperature corrected average ER values of the four representative layers for both segments 1+2 and for all four performed measurements of S1 and S2.

Section	Layer	Average ER values [$\Omega \cdot m$]	
		fine sand coating Segment 1 (6-14 m)	fine sand + bentonite coating Segment 2 (16-24 m)
S1 (above EAHE)	Topsoil	70.72	48.17
	Coating layer	141.54	69.06
	Bedding layer	203.56	117.50
	Bottom Soil	194.82	129.49
S2 (reference)	Topsoil	37.92	34.71
	Coating layer	52.65	58.57
	Bedding layer	108.06	74.69
	Bottom Soil	200.65	107.36

308

309

310

311

312

313

314

315

316

317

318

319

320

321

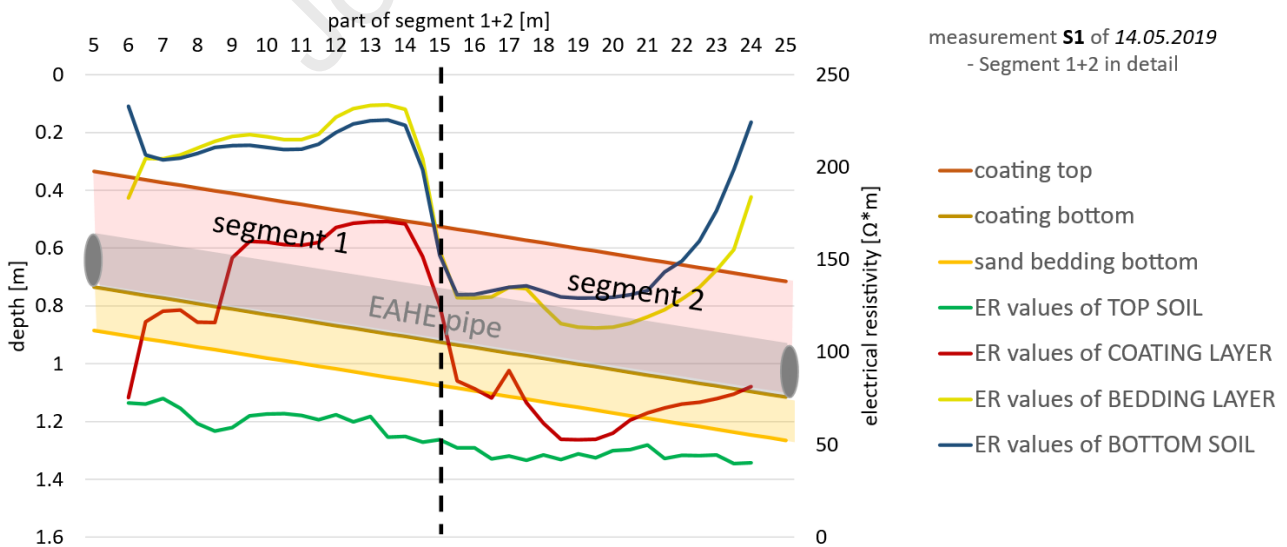
322

323

It becomes clear that the ER values within the relevant depth are generally higher within the EAHE area than within the natural soil conditions. This is particularly evident in the first segment, where differences of $\Delta = 88.9 \Omega \cdot m$ and $\Delta = 95.5 \Omega \cdot m$ occur within the Coating Layer and the Bedding Layer respectively. Regarding the second segment the highest difference shows up in depth of the Bedding layer ($\Delta = 42.8 \Omega \cdot m$), and the differences within the other layers are less than $\Delta < 22 \Omega \cdot m$. Hence, the ER values of the second segment in S1 correspond more to the natural state represented by S2. Concerning the Bottom soil, which is the same soil type for both S1 and S2, the ER values are very similar between the two sections. For example a little difference of $5.8 \Omega \cdot m$ is observed at segment 1 between S1 and S2.

Thus, the result reflects a disturbance of the upper three layers due to the EAHE installation and the Bottom soil layer corresponds approximately to the reference values.

3.3 Comparison of coating segments at EAHE installation section S1



324

Figure 10 : ER results corrected by temperature and merged for each layer of the S1 measurement of may in the range of the investigated coating layer segments of the EAHE installation and their respective depth.

325
326 For defining the influence of the different coating materials in first instance the difference between
327 segment 1 and segment 2 regarding the ER values of S1 must be highlighted (Figure 10). There, the
328 Topsoil ER is quite stable in comparison with the other three layers (Coating Layer, Bedding Layer,
329 Bottom Soil). Within the other three layers, a significant shift from segment 1 to segment 2 becomes
330 apparent.

331

332 3.4 Impact of seasonal soil temperature variation

333

334 For analysing the impact of the changing soil conditions by season, the ER values of the February
335 ERT measurements are compared with the values from May (Figure 11 and Appendix). As a
336 background information the seasonal soil temperatures for the Coating Layer are given (February:
337 8 °C; May: 13 °C). Corrected ER values decrease due to a correction at temperatures below 25 °C.
338 With the temperatures used correction factors of $f_{T_{\text{may}}}=1.31$ and $f_{T_{\text{feb}}}=1.49$ were determined for EC.
339 With regard to the resistivity values, this 5 °C temperature variation results in a difference of approx.
340 18 $\Omega\cdot\text{m}$ when applying an initial value of 200 $\Omega\cdot\text{m}$, which represents a difference of almost 10 %.
341 This goes in conformity with empirical linear approximations of 1.8 to 2.2 percent change in bulk
342 electrical conductivity per degree C (Hayley et al. 2007).

343

344 Regarding the uncorrected results for Section S1, the highest differences between February and may
345 (mostly above 20 %) occur within the upper two Layers (Topsoil and Coating Layer). Whereby this
346 effect is more distinct within the Segment with fine sand and bentonite (> 23 %). In this case the
347 seasonal deviations within the Bedding Layer and the Bottom soil are less than 6 %. For Section S2
348 on the reference area, the uncorrected results also show the same tendency even more clearly with
349 distinctly higher deviations within the Topsoil and the depth of the Coating Layer (> 26 %) and less
350 differences in the deeper Layers (< 16 %).

351

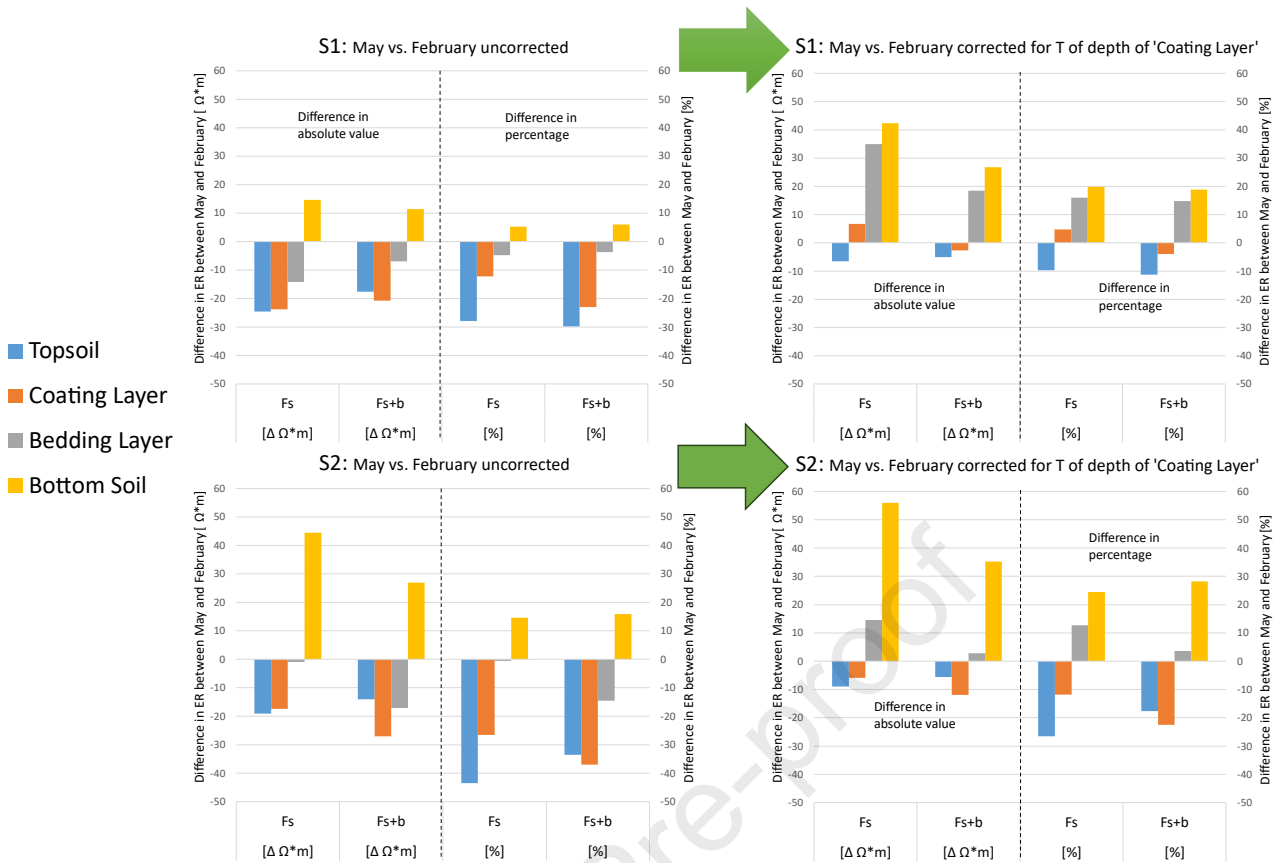
352 After the application of the temperature correction there is a shift in deviations between the layers
353 examined. Regarding the Section S1, that represents the ERT measurement directly upon the EAHE
354 system, now the least deviations occur within the Coating Layer (< 4.7 %). Concurrently, the Topsoil
355 above and the other two Layers below show higher seasonal effects now (Topsoil: 9.7-11.3 %;
356 Bedding Layer: 14.8-16.0 %; Bottom Soil: 18.9-19.8 %). In contrast to the uncorrected results, there
357 is no significant difference between both Segments to be found.

358

359 Within the corrected results for Section S2, the trend that the second layer has by far the lowest values
360 is not so clear. In this case the deviations between May and February vary more. Still, within the
361 depth of the Coating Layer and the Bedding Layer there are lower difference by average (Coating
362 Layer $\Delta_{\text{av}} = 17.2$ %; Bedding Layer $\Delta_{\text{av}} = 8.2$ %) than above (Topsoil: $\Delta_{\text{av}} = 22.1$ %) and below
363 (Bottom Soil: $\Delta_{\text{av}} = 26.4$ %). But in this instance the least deviations are within the Bedding Layer
364 and not within the Coating Layer as determined in Section S1.

365

366 Regardless of the temperature correction and the respective ERT measurement (S1, S2), the measured
367 ER values in February are almost always higher in the top two layers and lower in the bottom soil
368 than in May. By applying the temperature correction there is a reversal of values just within the
369 Bedding Layer. For this layer ER values are throughout higher in February before the correction and
370 after the correction the ER values are higher in May.



371

Figure 11: Comparison of February and May ER values once corrected by temperature and once not, to highlight the seasonal impact in the course of both measured ERT sections (S1+S2)

372

373

3.5 Impact of EAHE system running

374

375

376

377

378

379

380

381

To examine the impact of the running EAHE system, the data of the first measurement day of each measurement campaign, when the very shallow geothermal system was still running, is compared with the similarly performed ERT measurements on the next day, after the EAHE system was shut down in the evening before. Moreover, to evaluate the influence of the system, the differences between the first and second day were considered for both Sections, S1 and the reference S2 (Table 2). If an effect of the EAHE system is present, it should occur in S1, whereas only natural noise can be detected in S2.

382

383

384

385

386

387

388

Regarding the difference between both measurement days, the absolute changes are very small ($\Delta < 9.4 \Omega \cdot m$). Within installation depth (Coating Layer) of S1 the differences in Segment 1 with the fine sand coating are distinctly higher than the change of ER within Segment 2 (Coating Layer S1 $\Delta_{fs} = 5.0 \%$; $\Delta_{fs+b} = 1.3 \%$). Also, in comparison with the measured ER in Section S2 the change are less within the first Segment area. But in the area of Segment 2 of the Section S2 measurement, there are also deviations of more than 5 %, although the absolute value is a little bit less.

389

390

391

392

393

It has to be considered, that the performed temperature correction has no influence on the result in this case, since in this data analysis the differentiation of ER values is always made between measurements of the same measurement campaign (February or May). Thus, the compared ER values in each case are corrected with the same correction factor.

Table 2 : Mean differences as absolute values of ER values [$\Omega\cdot m$] corrected by temperature and as differential in percentage between first day and second day measurements to showcase the impact of EAHE system within S1 in comparison to S2

Segment	Impact of EAHE		Background noise	
	Results for Fs and Fs+b for S1 (running – not running)		Results for Segments Fs and Fs+b for reference S2 (first day – second day)	
	Fs [$\Omega\cdot m$ (%)]	Fs+b [$\Omega\cdot m$ (%)]	Fs [$\Omega\cdot m$ (%)]	Fs+b [$\Omega\cdot m$ (%)]
Topsoil	-3.9 (5.8 %)	-2.0 (4.2 %)	-1.3 (3.5 %)	-1.4 (4.2 %)
(Depth of) Coating Layer	-6.9 (5.0 %)	0.9 (1.3 %)	-1.4 (2.6 %)	-3.2 (5.7 %)
(Depth of) Bedding Layer	-5.2 (2.6 %)	3.8 (3.1 %)	0.1 (0.1 %)	1.2 (1.5 %)
Bottom Soil	-1.8 (1.1 %)	2.3 (1.6 %)	4.3 (2.1 %)	9.4 (7.7 %)

394

395 -4. Discussion

396 Soil conditions and the thermal characteristics of the grouting material are essential for the
 397 performance of near-surface geothermal energy. With variation in soil properties and grouting
 398 material the needed space for a very shallow geothermal installation to cover a distinct demand for
 399 heating or cooling is affected. Within the study of Lin et al.[55] the impact of water content on the
 400 energy performance of an EAHE was already investigated. Furthermore, the impact of the different
 401 grouting materials was analysed [8, 9].

402
 403 But is it still possible to check afterwards whether the correct material was used? In order not to cause
 404 any damage, only non-invasive measuring methods like ERT measurements can be used. To define
 405 relevant soil properties for very shallow geothermal potentials ERT measurements can be used as a
 406 tool. However, ERT measurements determine the electrical conductivity and the soil properties are
 407 'only' derived from the measured results. If the ERT measurement is affected by varying influencing
 408 parameters which are not taken into account, this can lead to incorrect derivations or misjudgements.
 409 It is therefore essential to take a close look at the influence of the changing parameters with season
 410 on the ERT measurement to be able to make the right conclusions in the end. The following discussion
 411 points mainly deal with the determination of the soil and grouting material and the influence of
 412 temperature from different sources to analyse the weaknesses and possibilities of the used
 413 methodology.

415 4.1 Classification of soil and of the grouting material by ER values

416 In general, finer-grained soils exhibit lower ER than coarse-grained soils [21, 29]. Regarding the
 417 investigated soil in this study, besides the solum the natural soil profile consists almost entirely of
 418 soil layers characterised by gravel with only few fine-grained horizons. The granulometric analysis
 419 of a gravel layer exhibits that more than 60 % of the natural soil backfilling material consists of gravel
 420 and a total of 20 % correspond to grain sizes of medium and coarse gravel ($\emptyset > 10$ mm). Due to the
 421 original coarse soil material ER values are rising distinctly over $100 \Omega\cdot m$. According to the GGU [60]
 422 saturated sand and gravel are around $50\text{--}200 \Omega\cdot m$. Just moist gravel has already values $>1000 \Omega\cdot m$.
 423 With values above $200 \Omega\cdot m$ throughout the profile below the installation depth it is clear, that the
 424 original soil texture is very coarse.

425 In contrast to the coarse-grained soil textures, within the EAHE installation the added coating material
 426 defined as a fine sand has no gravel content and in the case of segment 2 additionally a small amount
 427 of fine-grained soil material (≈ 10 %) comes on top. For silt soil for example, a range of 20 to 100
 428 $\Omega\cdot m$ is given as a rough recommendation. This is mainly due to the sensitivity of the ERT
 429 measurements in relation to the soil water content, which is generally higher in finer-grained soils
 430 [20, 21, 25].

431 Hence, it would be expected that the ER in Segment 2 (fs+b) would be lower than in Segment 1 (fs)
432 and the values in the whole area of the grouted GSHE would be lower than those in the same depth
433 of the reference measurement S2. This rough assumption is reflected in the results of the geoelectric
434 investigation (Figure 8, Figure 9). One might have expected that a layer with bentonite would have
435 even lower ER values than such a gravelly loam like the initial soil. But in this case the amount (\approx
436 10 %) is not sufficient to obtain clay specific ER values that are below 20 $\Omega\cdot\text{m}$.

437 Regarding the ERT measurement itself, the performed electrode spacing of 0.5 m should ensure an
438 optimal adapted spatial resolution, since Dumont, Pilawski, Hermans, Nguyen and Garré [23] also
439 tested different electrode spacings and have recommended an electrode spacing of 0.5 m for the best
440 possible resolution at the investigated depth. Although, characterisation of ERT results must be taken
441 with caution [61].

442
443 For the further discussion it has to be considered, that in partial areas this ascertained installation
444 depth of the Sand Beddings lower bound can be deeper than in theory. At the soil-probing point within
445 segment 2 a divergence was found. Whereas the theoretical thickness of the bedding sand layer should
446 be 0.15m, the actual measured thickness is about 0.34 m [8].

448 4.2 Comparison between initial field conditions and the geothermal installation

449 It was found that the ER values within the installation depth are generally higher within S1 than in
450 the initial field conditions of S2. It is unclear whether the installed heat exchanger pipe itself has an
451 influence on the ER values of the Coating Layers of S1. This could possibly also increase the ER of
452 S1 somewhat.

453 In detail it has to be considered, that the natural soil profile shows a loamy layer with a small subjacent
454 clay layer in the same depth at which the EAHE system was installed (Figure 3). This explains that
455 the ER values in the reference measurement S2 in the depths of Coating Layer and Bedding Layer
456 (Table 1) correspond to ER values of loamy or silty soil. ER values only increase to 'gravelly' values
457 in the Bottom Soil Layer. The ER values of the natural soil (S2) at the depth level of Coating Layer
458 are therefore converging to the values of the coating material with the bentonite addition in Segment
459 2 of S1. Hence, the ER values of the grouting material of the second segment correspond more to the
460 natural state, due to the loamy and clayey layers present within installation depth.

461 Since the fine-grained component is missing in the grouting material (Coating Layer) of Segment 1
462 as well as within the Bedding Layer of both Segments, higher ER values within section S1 are
463 significant in these domains.

464 With regard to the differences between all four investigated Layers, the result reflects a disturbance
465 of the upper three layers, ascertained by elevated ER values, due to the EAHE installation. But the
466 Bottom Soil Layer corresponds approximately to the reference values.

468 4.3 Comparison of coating segments

469 The measured ERT section S1 (Figure 8 and Figure 10) shows, that the two grouting segments of
470 only fine sand and fine sand with bentonite can be distinguished, clearly.

471
472 With regard to the average ER values for the investigated Layers of Section 1 (Figure 10), ER of
473 Segment 1 with only fine sand is significantly and throughout higher than the ER values of the
474 Segment 2 with fine sand and bentonite. This result is still true also a small shift between both
475 segments could already occur because the represented domains are descending with the slope of the
476 EAHE installation.

477
478 Taking the reference measurement S2 into account it shows clearly that the deviation within the
479 Coating Layer must be due to the different coating materials, because within the same depth in S2 the
480 ER values are even lower than in Segment 2 of S1 and they are very steady.

481 The difference between both installed grouting materials was to be expected, because the addition of
482 a fraction of fine grains to a pure sand. Although the bentonite addition is just around 10 %, it changes

483 its physical soil properties and primarily the water retention capacity [62]. And due to the sensitivity
484 of ERT with respect to water content [20, 21, 25], this change in soil texture could have been resolved
485 very clearly.

486
487 The difference between both grouting segments is most evident in the Coating Layer
488 ($\Delta_{\text{Coating_Layer}} = 51.1\%$) and the Bedding Layer ($\Delta_{\text{Bedding_Layer}} = 42.2\%$), but there are also differences
489 around 30 % in in the Bottom Soil. With that the difference in the Bottom Soil almost reaches the
490 same proportions as the Layers of the installed EAHE system. Regarding the Topsoil the absolute
491 difference ($\Delta_{\text{Topsoil}} = 22.6 \Omega\cdot\text{m}$) is lower than within the other Layers and on the contrary to all deeper
492 layers no distinct change between both segments is detected (Figure 10).

493
494 It seems that the impact of the different soil textures considering the respective grouting materials
495 also affects the surrounding ERT results. Regarding the mean ER values in Topsoil, generally they
496 are also higher than in the reference area and they decrease gradually from segment 1 to segment 2,
497 although the reference indicates a steady state under natural conditions. Although, there is no
498 significant transition between the ER of both segments in the Topsoil, it may be, that due to these
499 different grouting materials or rather soil textures of the EAHE Coating Layers, soil of the layer above
500 is also affected. The influencing factor could be the fact, that the soil material with a small amount of
501 bentonite incorporated in segment 2 has higher water-holding capacity which may influence also
502 saturation of the Topsoil Layers.

503
504 This influence of the Coating material on the surrounding layers is even more pronounced in the
505 Bedding Layer and Bottom Soil, where ER values are distinctly higher in the area of Segment 1 than
506 in the area of Segment 2 (Figure 10).

507 Although, the Wenner array has generally a relatively low noise contamination, sometimes the spatial
508 resolution is reduced [58]. Dumont, Pilawski, Hermans, Nguyen and Garré [23] have also stated a
509 shift of the ER results to larger depths of around 0.5 m at an investigation depth similar to the
510 installation depth of the EAHE system. Thus, it is therefore possible that, in addition to the influence
511 of the modified soil texture above, ER processing also has an influence on the lower layers.

512
513 With regard to the reference ERT measurement S2, where the same data accumulation was carried
514 out, no significant changes in the Topsoil Layer were achieved. In S2 first notable differences occur
515 in depth of the Bedding layer and become distinct in the Bottom Soil layer. Thus, the shift of ER
516 values in the upper two layers between Segment 1 with fine sand and Segment 2 with fine sand and
517 bentonite is unambiguously due to the different Coating materials, whereas the shift beneath the
518 installation within the Bottom Soil can also be partly attributed to pre-existing natural conditions.
519 Nevertheless, the different grouting materials show their influence because the change of ER in the
520 Bottom Soil layer is very clear at the transition between both segments (Figure 10).

521
522 Furthermore, it is shown that differences within grouting material can be detected, which enables the
523 possibility for controlling the backfilled grouting material of a very shallow geothermal system after
524 installation by using non-invasive ERT measurements. The right grouting material may be crucial for
525 an increased energy performance and with that a diminution of a needed tube length [8].
526

527 4.4 Seasonal temperature variation

528

529 Regarding the results compared between February and May, the influence of soil temperature on ER
530 cannot be denied. In order to determine the influence of the seasons, the corrected and not corrected
531 measurements from February were compared with those taken in May.

532 Regarding the not corrected ER values (Figure 11), the contrast between February and May is more
533 significant within the near surface layers and the differential decreases with depth. This is true for
534 both measured sections (S1 and S2), although this trend is more pronounced in the reference
535 measurement S2. Thus, within the Topsoil and the Coating Layer there are the highest percentage
536 deviations of ER between February and May, whereas the deviations in the depth of the Bedding
537 Layer and the Bottom Soil vary less. This also applies to the absolute difference of ER, although this
538 trend is not as significant then, due to the fact that the measured ER for the deeper layers is at higher
539 values.

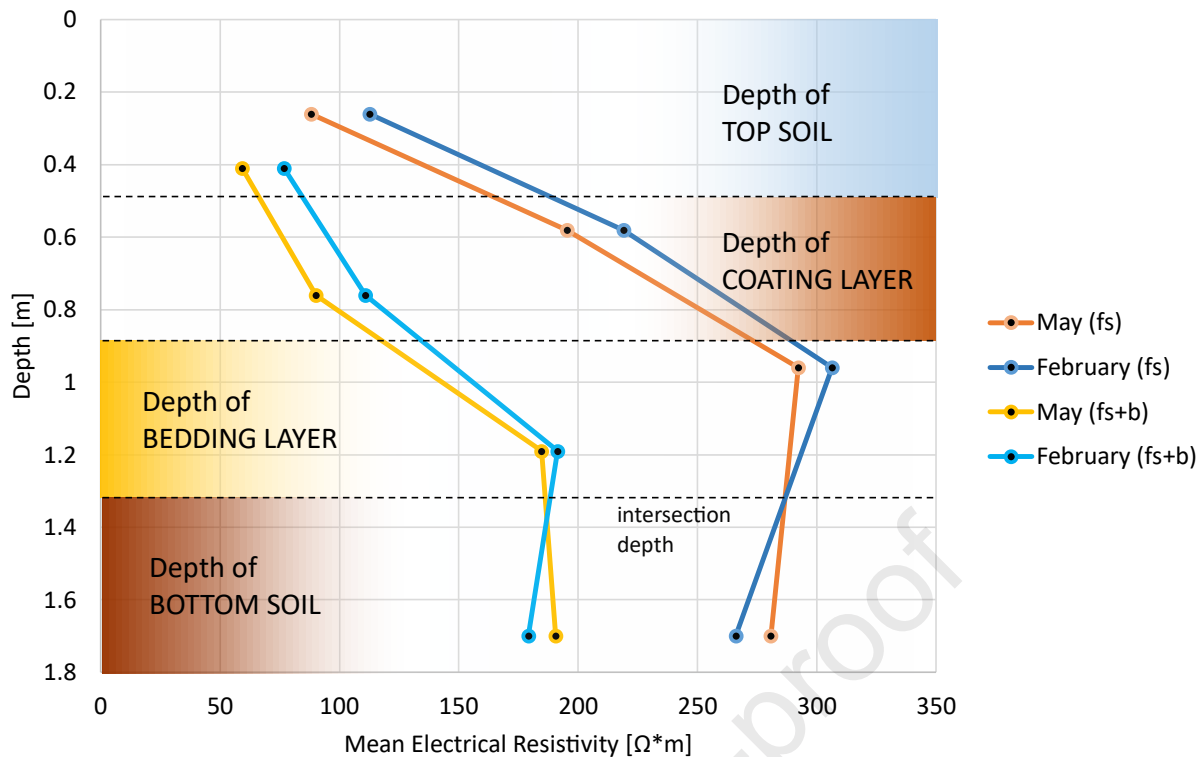
540 As the year progresses, soil temperatures change and this change of temperature decreases with depth
541 [27, 63]. Hence, this measured ERT variation between February and May is generally consistent with
542 the seasonal temperature spread decreasing with depth. The variations of ER are highest in Topsoil
543 and decrease with depth.

544 It should be noted, that the sign of the differentials is reversed in the Bottom Soil layer (Figure 12).
545 Thus, the measured ER within the depth range of the EAHE installation (Topsoil, Coating Layer,
546 Bedding Layer) are consistently higher in February than in May. But within the Bottom Soil Layer
547 this changes and ER are higher in May.

548 That within the cold season higher ER within the near surface layers occur correspond to the general
549 context that colder soil material refers to increased ER, as described by the temperature correction
550 models [19, 31]. But this change of the differential sign in the Bottom Soil layer regarding the ER
551 values indicates that also the temperature difference might be changed in this depth or another factor
552 than temperature like soil moisture has impact on the ER results. It might be that the soil moisture in
553 February is a little higher than that in May. This can be explained ancillary by the antecedent
554 precipitation recorded on the test site. The 7-days antecedent cumulated precipitation before the test
555 in February is 30 mm, while that before the test in May is 16 mm.

556 But, compared to observed temperature-depth profiles by Bense and Kooi [63] still in June soil
557 temperatures decrease within 3-4 meters below temperatures measured in January. In February
558 temperature in this depth will be lower and in May temperature won't have risen as much as in June.
559 Thus, if we assume that temperature is the only influencing factor it is still conceivable, that this
560 intersection of both temperature-depth profiles of February and May is around almost 1.5 m due to
561 the delayed temperature response with depth.

562



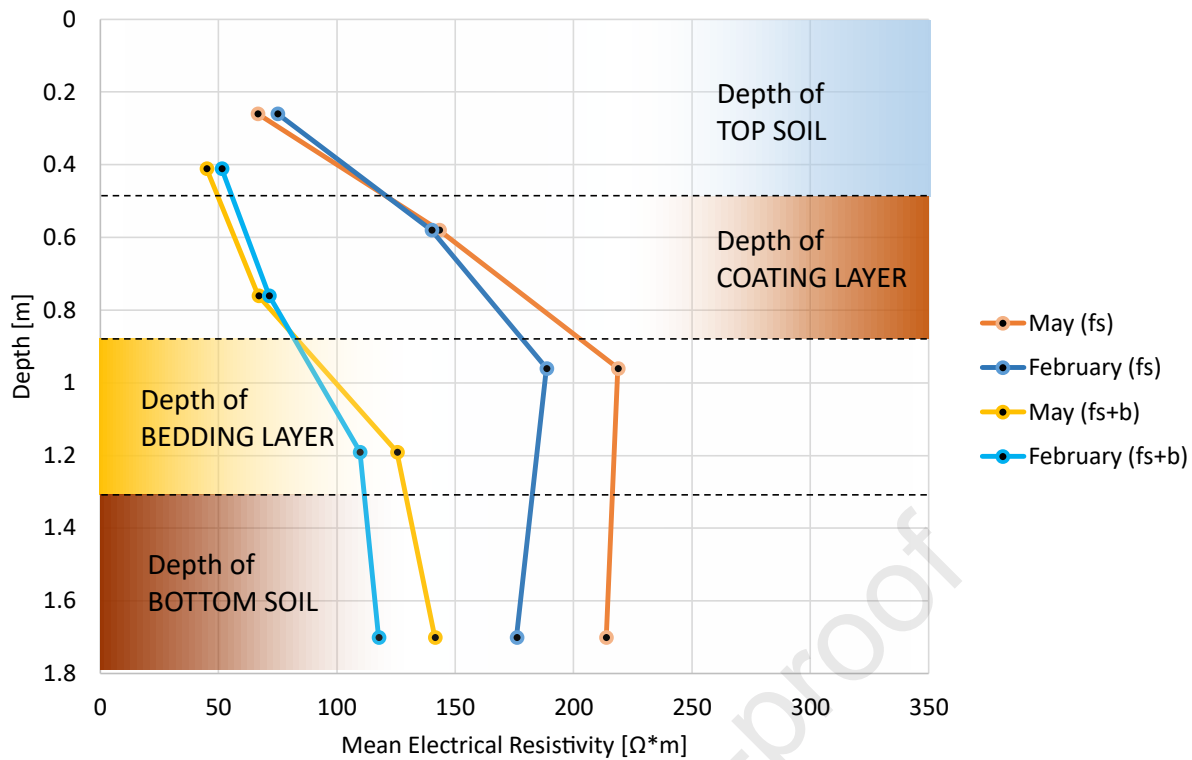
563

Figure 12 : Not corrected mean ER values. Profiles of Section 1 (above the EAHE installation) for February and May and for each Segment respectively.

564 On the other hand, this intersection of the ER differential between the values of February and May in
 565 a depth of around 1.4 m could be the indication for another influencing factor like variations in soil
 566 moisture. Soil moisture has a variable characteristic through season within the unsaturated soil
 567 column which could be detected also by ERT measurements due to its high sensitivity regarding water
 568 content. Generally, higher soil water content results in an increased electrical conductivity and with
 569 that in a decreased ER [21, 25]. It should be assumed that soil moisture in February is higher than in
 570 May. If the seasonal impact in ER is driven by soil moisture in February a reduced ER would be
 571 expected. But in this case the February ER values are higher within the upper layers. This indicates
 572 that at least at depths down to approx. 1.4 m the seasonal changes in ER are driven by temperature
 573 and not by soil moisture. However, it is not yet clear whether soil temperature in the direct subsurface
 574 of the investigated test area is the only influencing factor or if soil moisture has also its effect. But
 575 regarding the conversion of the Bedding Layer, after temperature correction it can be assumed that
 576 the soil moisture has an increased influence within the lower layers investigated, especially if the
 577 precipitation values from the previous week before the respective measurement are taken into
 578 account.

579
 580 To really prove the impact of soil moisture over season another ERT measurements should have had
 581 performed within the late summer, because from winter until June the monitored soil moisture (Figure
 582 4) is fluctuating around 20 %, which represents the effect of the humid period. The effect of the
 583 summer drought does not decrease soil moisture to approx. 10 % until the end of June. Thus, the
 584 measurement period could not cover the complete range of soil moisture variation within the
 585 installation depth of the test-site.

586



587

Figure 13: Mean ER values corrected by temperature. Profiles of Section 1 (above the EAHE installation) for February and May and for each Segment respectively.

588

589

590

591

592

593

It is interesting to note that by applying this temperature correction of the ER (Figure 13) the seasonal differences become minimal within the Coating Layer especially in S1. Thus, as a consequence of a correction by temperature measured at the heat exchanger depth, shifts the intersection depth upwards to exactly the depth where the temperature for correction was measured.

594

595

596

597

598

599

In S2 this intersection depth varies between the Coating Layer and the Bedding Layer. It must be taken into account that the temperature correction was carried out solely on the basis of a single temperature for this depth level of the Coating Layer and not for an entire temperature profile. This also means that the temperature correction for the Coating Layer was calculated with suitable temperatures, but since the same the temperature is used for the other layers, correction probably deviates from the natural circumstances.

600

601

602

603

604

The result shows that the temperature correction of ER counteracts the seasonal effect. Even though this is not necessarily surprising, since representative temperatures for the respective month were used for ER correction. In (long-term) ERT studies, it is therefore important to consider the effect of a temperature correction on the scientific question of the study.

605

606

607

608

609

610

611

612

613

As a further result this study shows that seasonal ERT investigations can enable conclusions about the influence of soil temperature within different depth layers through the year, although, it is suggested that measuring of temperature changes by ERT measurements can be challenging [46, 64, 65]. Arato, Boaga, Comina, De Seta, Di Sipio, Galgaro, Giordano and Mandrone [41] also pointed out this issue especially in unsaturated zones. Usually, temperature effects can be measured by ERT, but particularly when relative temperature differences are large [29]. But in this case a seasonal temperature impact of a difference within installation depth (depth of Coating Layer) of around 5 degrees could have been detected by resistivity measurements.

614 4.5 EAHE running impact

615 Regarding the impact of the EAHE system operation itself no significant effect was identified. Still,
616 it seems to be visible within the segment with only fine sand, because there the highest absolute
617 differences occur within the Coating and Bedding Layer in the results of S1. There, the ER values on
618 the first day are consistently lower than on the second day. This is true for May and February as well.
619 Regarding the second segment with fine sand and bentonite as a grouting material nearly no
620 deviations occur. Furthermore, the results between running and not running the system do not differ
621 to a significantly greater extent as the deviations within the reference, which should represent the
622 background noise. Thus, a significant impact of the EAHE impact could not have been achieved after
623 12 h within this measurement setting.

624 It has to be considered that in contrast to other studies, the temperature emitted is quite low in this
625 case. This is due to the fact, that this installation consists of only one single pipe and not of a pipe
626 accumulation like within a trench collector. Moreover, for this approach no high air velocity was
627 applied, especially. Thus, also no high temperatures were applied on the system like other approaches
628 did [28, 47]. A higher air velocity within the EAHE system might have had a more significant
629 difference as a result.

630
631 In this case, the impact of the EAHE installation is mainly present due to the changed soil type in the
632 Coating and Bedding Layer and not due to the operation of the system.
633

634 -5. Conclusions

635
636 The aim of the study to assess relevant soil texture and grouting material characteristics with regard
637 to very shallow geothermal systems by using ERT measurements was successfully reached. By
638 applying ERT a fast area-wide investigation with focus on the relevant influencing parameters for
639 very shallow geothermal potential estimations can be carried out. One advantage of this non-invasive
640 measurement method is that tests can also be carried out after the GSHE has been installed. This also
641 allows the grouting material to be inspected with regard to its thermal properties. Nevertheless, the
642 investigated influence of temperature also shows the challenges of the methodology
643

644 First of all, relative homogeneous natural soil conditions were found within the reference soil section
645 S2, although in installation depth there are mediate ER values due to some more fine-grained layers
646 within the context of a soil profile dominated by gravelly soil.
647

648 Regarding the soil section S1 where the GSHE is buried, the influence of the used grouting materials
649 on the ER was ascertained. The ERT measurement shows that the upper three layers (Topsoil, Coating
650 Layer, Bedding Layer) are disturbed by the EAHE installation, whereas the Bottom Soil is in
651 accordance with the natural conditions. Thus, the depth of disturbance was identified. The difference
652 in ER between a grouting material of only fine sand and a second grouting material of the same sand
653 and 10 % bentonite is significant. With regard to the Coating Layers of segment 1 and 2 of S1 this
654 change in grouting material causes a shift of approx. $70 \Omega \cdot m$.
655

656 By comparing ER values between the two tests in February and in May, it has been shown that the
657 temperature correction of ER values is necessary to evaluate the impact of temperature and to get a
658 consistent analysis about the soil moisture in the field. The corrected ER result shows that the
659 temperature correction of ER counteracts the seasonal effect, which underlines the sense of the
660 correction. In fact, ER values without temperature correction could also indicate that the soil moisture
661 in February is lower than that in May for all the soil layers. But by applying the temperature correction
662 a similar soil moisture level until Coating Layer between the two tests has been found. Furthermore,
663 ER values with temperature correction show a more humid bottom layer in February, which is
664 supported by the recorded precipitation on the site.

665
666 Finally, little impact of the EAHE operating has been detected by ERT measurements. This means
667 that ERT tests could be carried out when the EAHE system is still running.

668
669 This study shows furthermore, that ERT measurements enable an ideal assessment of the essential
670 soil and grouting material characteristics for evaluation of subsurface installations that are depending
671 on heat propagation or thermal properties of soil like very shallow geothermal applications or high
672 voltage underground cable constructions. Especially with regard to soil type, soil moisture and of
673 cause temperature variations, ERT measurements are a valuable tool in this context.

674
675
676 Acknowledgements:

677
678 We are thankful that we could use the test-site with the EAHE installation of the University of
679 Strasbourg at the ICUBE(UMR7357), IUT Robert Schuman. Further, we thank our colleague Jan
680 Wagner for assistance in the course of our field measurements.

681
682 Funding:

683
684 This study was supported by BayFrance, the university centre for Bavarian-French scientific
685 cooperation (FK19_2018).

686
687 Authorship contribution statement:

688 **Hans Schwarz:** Data curation, Formal analysis, Investigation, Methodology, Validation,
689 Visualization, Roles/Writing - original draft. **Jian Lin:** Conceptualization, Investigation,
690 Methodology, Project administration, Validation, Writing - review & editing. **David Bertermann:**
691 Conceptualization, Project administration, Resources, Funding acquisition, Supervision

692
693 **References**

- 694
695 [1] T. Amanzholov, A. Seitov, A. Aliuly, Y. Yerdesh, M. Murugesan, O. Botella, M. Feidt, H.S. Wang, Y.
696 Belyayev, A. Toleukhanov, Thermal Response Measurement and Performance Evaluation of Borehole Heat
697 Exchangers: A Case Study in Kazakhstan, *Energies* 15(22) (2022) 8490.
- 698 [2] O. Suft, D. Bertermann, One-Year Monitoring of a Ground Heat Exchanger Using the In Situ Thermal
699 Response Test: An Experimental Approach on Climatic Effects, *Energies* 15(24) (2022) 9490.
- 700 [3] S. Wilke, K. Menberg, H. Steger, P. Blum, Advanced thermal response tests: A review, *Renewable and*
701 *Sustainable Energy Reviews* 119 (2020) 109575.
- 702 [4] R. Al-Khoury, N. BniLam, M.M. Arzanfudi, S. Saeid, Analytical model for arbitrarily configured
703 neighboring shallow geothermal installations in the presence of groundwater flow, *Geothermics* 93 (2021)
704 102063.
- 705 [5] M.L. Fasci, A. Lazzarotto, J. Acuña, J. Claesson, Simulation of thermal influence between independent
706 geothermal boreholes in densely populated areas, *Applied Thermal Engineering* 196 (2021) 117241.
- 707 [6] H. Schwarz, N. Jovic, D. Bertermann, Development of a Calculation Concept for Mapping Specific Heat
708 Extraction for Very Shallow Geothermal Systems, *Sustainability* 14(7) (2022).

- 709 [7] Y. Zhou, A. Bidarmaghz, N. Makasis, G. Narsilio, Ground-source heat pump systems: The effects of
710 variable trench separations and pipe configurations in horizontal ground heat exchangers, *Energies* 14(13)
711 (2021) 3919.
- 712 [8] M. Cuny, J. Lin, M. Siroux, V. Magnenet, C. Fond, Influence of coating soil types on the energy of earth-
713 air heat exchanger, *Energy and Buildings* 158 (2018) 1000-1012.
- 714 [9] M. Cuny, J. Lin, M. Siroux, C. Fond, Influence of an improved surrounding soil on the energy
715 performance and the design length of earth-air heat exchanger, *Applied Thermal Engineering* 162 (2019)
716 114320.
- 717 [10] E. Di Sipio, D. Bertermann, Factors influencing the thermal efficiency of horizontal ground heat
718 exchangers, *Energies* 10(11) (2017) 1897.
- 719 [11] L. Mascarin, E. Garbin, E. Di Sipio, G. Dalla Santa, D. Bertermann, G. Artioli, A. Bernardi, A. Galgaro,
720 Selection of backfill grout for shallow geothermal systems: materials investigation and thermo-physical
721 analysis, *Construction and Building Materials* 318 (2022) 125832.
- 722 [12] F. Delaleux, X. Py, R. Olives, A. Dominguez, Enhancement of geothermal borehole heat exchangers
723 performances by improvement of bentonite grouts conductivity, *Applied Thermal Engineering* 33 (2012) 92-
724 99.
- 725 [13] VDI_4640-2, VDI 4640 Part 2 - Thermal use of the underground - Ground source heat pump systems,
726 in: V.D.I.e.V.V.-G.E.u.U. (GEU) (Ed.) Beuth Verlag GmbH, Düsseldorf, 2019.
- 727 [14] D. Bertermann, H. Klug, L. Morper-Busch, A pan-European planning basis for estimating the very
728 shallow geothermal energy potentials, *Renewable energy* 75 (2015) 335-347.
- 729 [15] D. Bertermann, H. Klug, L. Morper-Busch, C. Bialas, Modelling vSGPs (very shallow geothermal
730 potentials) in selected CSAs (case study areas), *Energy* 71 (2014) 226-244.
- 731 [16] D. Assouline, N. Mohajeri, A. Gudmundsson, J.-L. Scartezzini, A machine learning approach for mapping
732 the very shallow theoretical geothermal potential, *Geothermal Energy* 7(1) (2019) 1-50.
- 733 [17] I. Çağlar, M. Demirörer, Geothermal exploration using geoelectric methods in Kestanol, Turkey,
734 *Geothermics* 28(6) (1999) 803-819.
- 735 [18] R.F. Corwin, D.B. Hoover, The self-potential method in geothermal exploration, *Geophysics* 44(2)
736 (1979) 226-245.
- 737 [19] D.L. Corwin, S.M. Lesch, Apparent soil electrical conductivity measurements in agriculture, *Computers*
738 *and electronics in agriculture* 46(1-3) (2005) 11-43.
- 739 [20] S.P. Friedman, Soil properties influencing apparent electrical conductivity: a review, *Computers and*
740 *Electronics in Agriculture* 46(1-3) (2005) 45-70.
- 741 [21] D. Bertermann, H. Schwarz, Bulk density and water content-dependent electrical resistivity analyses of
742 different soil classes on a laboratory scale, *Environmental Earth Sciences* 77 (2018) 1-14.
- 743 [22] M. Chrétien, J. Lataste, R. Fabre, A. Denis, Electrical resistivity tomography to understand clay behavior
744 during seasonal water content variations, *Engineering geology* 169 (2014) 112-123.
- 745 [23] G. Dumont, T. Pilawski, T. Hermans, F. Nguyen, S. Garré, The effect of initial water distribution and
746 spatial resolution on the interpretation of ERT monitoring of water infiltration in a landfill cover, *Hydrology*
747 *and Earth System Sciences Discussions* (2018) 1-26.

- 748 [24] S. Kraxberger, D. Taferner, H. Klug, 3D Electrical Resistivity Tomography in the Mondsee Catchment,
749 *GI_Forum* 2017 5 (2017) 69-78.
- 750 [25] M. McCutcheon, H. Farahani, J. Stednick, G. Buchleiter, T. Green, Effect of soil water on apparent soil
751 electrical conductivity and texture relationships in a dryland field, *Biosystems Engineering* 94(1) (2006) 19-
752 32.
- 753 [26] H. Schwarz, D. Bertermann, Mediate relation between electrical and thermal conductivity of soil,
754 *Geomechanics and Geophysics for Geo-Energy and Geo-Resources* 6 (2020) 1-16.
- 755 [27] K. Hayley, L.R. Bentley, M. Gharibi, M. Nightingale, Low temperature dependence of electrical
756 resistivity: Implications for near surface geophysical monitoring, *Geophysical research letters* 34(18) (2007).
- 757 [28] T. Hermans, A. Vandenbohede, L. Lebbe, F. Nguyen, A shallow geothermal experiment in a sandy
758 aquifer monitored using electric resistivity tomography, *Geophysics* 77(1) (2012) B11-B21.
- 759 [29] M. Nouveau, G. Grandjean, P. Leroy, M. Philippe, E. Hedri, H. Boukcim, Electrical and thermal behavior
760 of unsaturated soils: experimental results, *Journal of Applied Geophysics* 128 (2016) 115-122.
- 761 [30] N. Giordano, C. Comina, G. Mandrone, Laboratory scale geophysical measurements aimed at
762 monitoring the thermal affected zone in Underground Thermal Energy Storage (UTES) applications,
763 *Geothermics* 61 (2016) 121-134.
- 764 [31] K.R. Sheets, J.M. Hendrickx, Noninvasive soil water content measurement using electromagnetic
765 induction, *Water resources research* 31(10) (1995) 2401-2409.
- 766 [32] N.H. Abu-Hamdeh, R.C. Reeder, Soil thermal conductivity effects of density, moisture, salt
767 concentration, and organic matter, *Soil science society of America Journal* 64(4) (2000) 1285-1290.
- 768 [33] D. Barry-Macaulay, A. Bouazza, R.M. Singh, B. Wang, P. Ranjith, Thermal conductivity of soils and rocks
769 from the Melbourne (Australia) region, *Engineering Geology* 164 (2013) 131-138.
- 770 [34] D. Bertermann, H. Schwarz, Laboratory device to analyse the impact of soil properties on electrical and
771 thermal conductivity, *International Agrophysics* 31(2) (2017).
- 772 [35] J. Côté, J.-M. Konrad, Thermal conductivity of base-course materials, *Canadian Geotechnical Journal*
773 42(1) (2005) 61-78.
- 774 [36] S.D. Logsdon, T.R. Green, J.V. Bonta, M.S. Seyfried, S.R. Evett, Comparison of electrical and thermal
775 conductivities for soils from five states, *Soil science* 175(12) (2010) 573-578.
- 776 [37] D.N. Singh, S.J. Kuriyan, K.C. Manthena, A generalised relationship between soil electrical and thermal
777 resistivities, *Experimental Thermal and Fluid Science* 25(3-4) (2001) 175-181.
- 778 [38] S. Sreedeeep, A. Reshma, D. Singh, Generalized relationship for determining soil electrical resistivity
779 from its thermal resistivity, *Experimental Thermal and Fluid Science* 29(2) (2005) 217-226.
- 780 [39] Q. Sun, C. Lü, Semiempirical correlation between thermal conductivity and electrical resistivity for silt
781 and silty clay soils, *Geophysics* 84(3) (2019) MR99-MR105.
- 782 [40] T. Tokoro, T. Ishikawa, S. Shirai, T. Nakamura, Estimation methods for thermal conductivity of sandy
783 soil with electrical characteristics, *Soils and foundations* 56(5) (2016) 927-936.
- 784 [41] A. Arato, J. Boaga, C. Comina, M. De Seta, E. Di Sipio, A. Galgaro, N. Giordano, G. Mandrone,
785 Geophysical monitoring for shallow geothermal applications-Two Italian case histories, *First Break* 33(8)
786 (2015) 75-79.

- 787 [42] C. Comina, N. Giordano, G. Ghidone, F. Fischanger, Time-lapse 3d electric tomography for short-time
788 monitoring of an experimental heat storage system, *Geosciences* 9(4) (2019) 167.
- 789 [43] M. Cultrera, J. Boaga, E. Di Sipio, G. Dalla Santa, M. De Seta, A. Galgaro, Modelling an induced thermal
790 plume with data from electrical resistivity tomography and distributed temperature sensing: A case study in
791 northeast Italy, *Hydrogeology Journal* 26(3) (2018) 837-851.
- 792 [44] C. Sáez Blázquez, I. Martín Nieto, A. Farfán Martín, D. González-Aguilera, P. Carrasco García,
793 Comparative analysis of different methodologies used to estimate the ground thermal conductivity in low
794 enthalpy geothermal systems, *Energies* 12(9) (2019) 1672.
- 795 [45] N. Giordano, A. Arato, C. Comina, G. Mandrone, Time-lapse electrical resistivity imaging of the
796 thermally affected zone of a Borehole Thermal Energy Storage system near Torino (Northern Italy), *Journal*
797 *of Applied Geophysics* 140 (2017) 123-134.
- 798 [46] T. Hermans, F. Nguyen, T. Robert, A. Revil, Geophysical methods for monitoring temperature changes
799 in shallow low enthalpy geothermal systems, *Energies* 7(7) (2014) 5083-5118.
- 800 [47] H. Schwarz, B. Badenes, J. Wagner, J.M. Cuevas, J. Urchueguía, D. Bertermann, A Case Study of Thermal
801 Evolution in the Vicinity of Geothermal Probes Following a Distributed TRT Method, *Energies* 14(9) (2021)
802 2632.
- 803 [48] M. Benhammou, B. Draoui, Parametric study on thermal performance of earth-to-air heat exchanger
804 used for cooling of buildings, *Renewable and Sustainable Energy Reviews* 44 (2015) 348-355.
- 805 [49] T.S. Bisioniya, A. Kumar, P. Baredar, Experimental and analytical studies of earth-air heat exchanger
806 (EAHE) systems in India: a review, *Renewable and Sustainable Energy Reviews* 19 (2013) 238-246.
- 807 [50] A. Mostafaeipour, H. Goudarzi, M. Khanmohammadi, M. Jahangiri, A. Sedaghat, H. Norouzianpour, S.
808 Chowdhury, K. Techato, A. Issakhov, K. Almutairi, Techno-economic analysis and energy performance of a
809 geothermal earth-to-air heat exchanger (EAHE) system in residential buildings: A case study, *Energy Science*
810 *& Engineering* 9(10) (2021) 1807-1825.
- 811 [51] C. Peretti, A. Zarrella, M. De Carli, R. Zecchin, The design and environmental evaluation of earth-to-air
812 heat exchangers (EAHE). A literature review, *Renewable and Sustainable Energy Reviews* 28 (2013) 107-
813 116.
- 814 [52] W. Zeitoun, J. Lin, M. Siroux, Energetic and Exergetic Analyses of an Experimental Earth-Air Heat
815 Exchanger in the Northeast of France, *Energies* 16(3) (2023) 1542.
- 816 [53] W. Zeitoun, J. Lin, M. Siroux, A Review-Earth-air Heat Exchanger: Applications, Advances and
817 Challenges, *IOP Conference Series: Earth and Environmental Science*, IOP Publishing, 2022, p. 012005.
- 818 [54] VDI_4640-4, VDI 4640 Part 4 - Thermal use of the underground - Direct uses, in:
819 Verein_Deutscher_Ingenieure_e.V. (Ed.) VDI-Gesellschaft Energie und Umwelt, 2004, p. 40.
- 820 [55] J. Lin, H. Nowamooz, S. Braymand, P. Wolff, C. Fond, Impact of soil moisture on the long-term energy
821 performance of an earth-air heat exchanger system, *Renewable Energy* 147 (2020) 2676-2687.
- 822 [56] M. Cuny, J. Lin, M. Siroux, C. Fond, Influence of rainfall events on the energy performance of an earth-
823 air heat exchanger embedded in a multilayered soil, *Renewable Energy* 147 (2020) 2664-2675.
- 824 [57] T. Dahlin, M.H. Loke, Resolution of 2D Wenner resistivity imaging as assessed by numerical modelling,
825 *Journal of applied geophysics* 38(4) (1998) 237-249.

- 826 [58] T. Dahlin, B. Zhou, A numerical comparison of 2D resistivity imaging with 10 electrode arrays,
827 Geophysical prospecting 52(5) (2004) 379-398.
- 828 [59] M.H. Loke, Tutorial: 2-D and 3-D electrical imaging surveys, (2004).
- 829 [60] GGU, Die Widerstandsgeoelektrik, 2011.
830 https://www.ggukarlsruhe.de/GGU_Die_Widerstandsgeoelektrik_WID98-C.pdf. (Accessed 16.02.2023
831 2023).
- 832 [61] C.-H.M. Tso, O. Kuras, P.B. Wilkinson, S. Uhlemann, J.E. Chambers, P.I. Meldrum, J. Graham, E.F.
833 Sherlock, A. Binley, Improved characterisation and modelling of measurement errors in electrical resistivity
834 tomography (ERT) surveys, Journal of Applied Geophysics 146 (2017) 103-119.
- 835 [62] K.E. Saxton, W.J. Rawls, Soil Water Characteristic Estimates by Texture and Organic Matter for
836 Hydrologic Solutions, Soil Science Society of America Journal 70(5) (2006) 1569-1578.
- 837 [63] V. Bense, H. Kooi, Temporal and spatial variations of shallow subsurface temperature as a record of
838 lateral variations in groundwater flow, Journal of geophysical research: Solid Earth 109(B4) (2004).
- 839 [64] T. Hermans, S. Wildemeersch, P. Jamin, P. Orban, S. Brouyère, A. Dassargues, F. Nguyen, Quantitative
840 temperature monitoring of a heat tracing experiment using cross-borehole ERT, Geothermics 53 (2015) 14-
841 26.
- 842 [65] T. Robert, C. Paulus, P.-Y. Bolly, E. Koo Seen Lin, T. Hermans, Heat as a proxy to image dynamic
843 processes with 4D electrical resistivity tomography, Geosciences 9(10) (2019) 414.
844

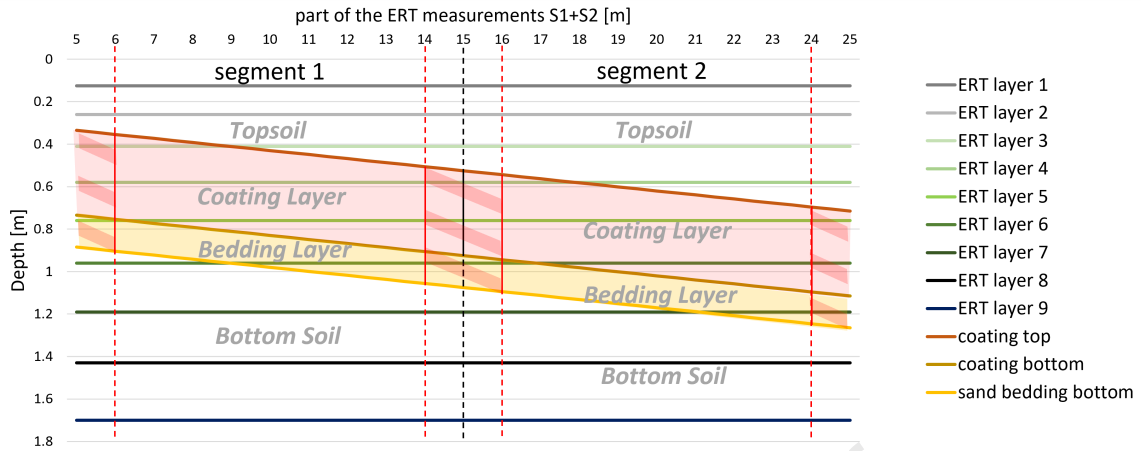
845 Appendix

Table 3 : Comparison of February and May ER values once corrected by temperature and once not, to highlight the seasonal impact in the course of ERT measurement **S1**.

Data status	Layer	ER values of May 2019		ER values of February 2020		Difference (May – February)			
		F _s [Ω*m]	F _{s+b} [Ω*m]	F _s [Ω*m]	F _{s+b} [Ω*m]	F _s [Δ Ω*m]	F _s [%]	F _{s+b} [Δ Ω*m]	F _{s+b} [%]
NOT corrected by tempera- ture	Topsoil	88.1	59.2	112.7	76.7	-24.6	-27.9	-17.6	-29.7
	Coating Layer	195.3	90.2	219.1	111.0	-23.8	-12.2	-20.7	-23.0
	Bedding Layer	292.2	184.6	306.3	191.5	-14.2	-4.8	-6.9	-3.7
	Bottom Soil	280.7	190.6	266.1	179.2	14.6	5.2	11.4	6.0
corrected by tempera- ture	Topsoil	66.5	45.0	74.9	51.4	-6.5	-9.7	-5.1	-11.3
	Coating Layer	143.1	66.8	140.0	71.3	6.7	4.7	-2.7	-4.0
	Bedding Layer	218.6	125.4	188.5	109.7	35.0	16.0	18.5	14.8
	Bottom Soil	213.7	141.3	175.9	117.6	42.4	19.8	26.8	18.9

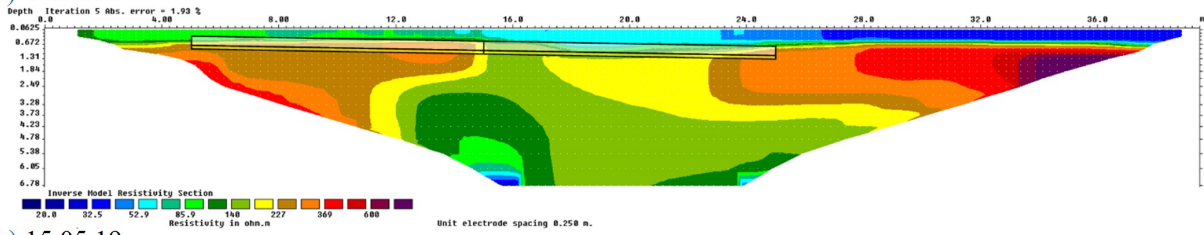
Table 4 : Comparison of February and May ER values once corrected by temperature and once not, to highlight the seasonal impact in the course of ERT measurement **S2**.

Data status	Layer	ER values of May 2019		ER values of February 2020		Difference (May – February)			
		F _s [Ω*m]	F _{s+b} [Ω*m]	F _s [Ω*m]	F _{s+b} [Ω*m]	F _s [Δ Ω*m]	F _s [%]	F _{s+b} [Δ Ω*m]	F _{s+b} [%]
NOT corrected by tempera- ture	Topsoil	44.0	41.9	63.2	56.0	-19.1	-43.5	-14.0	-33.5
	Depths of Coating Layer	65.7	72.9	83.2	99.9	-17.4	-26.5	-27.0	-37.0
	Depths of Bedding Layer	140.6	117.3	141.4	134.4	-0.9	-0.6	-17.1	-14.5
	Bottom Soil	304.2	169.1	259.7	142.2	44.4	14.6	26.9	15.9
corrected by tempera- ture	Topsoil	33.5	31.9	42.4	37.5	-8.9	-26.5	-5.6	-17.6
	Depths of Coating Layer	49.7	52.7	55.6	64.5	-5.9	-11.8	-11.9	-22.5
	Depths of Bedding Layer	115.4	76.1	100.8	73.3	14.6	12.7	2.8	3.6
	Bottom Soil	228.7	125.0	172.7	89.8	56.0	24.5	35.2	28.2

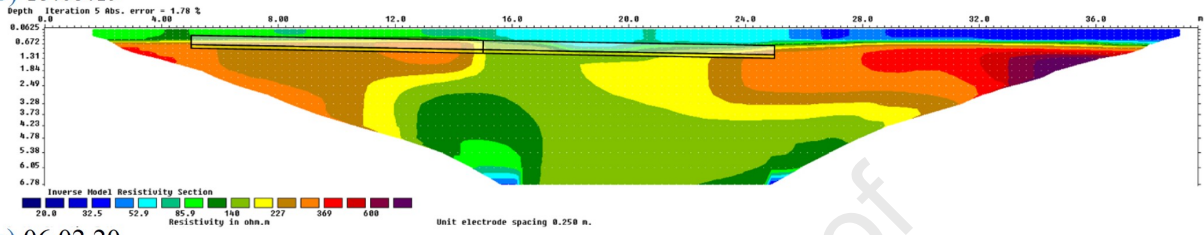


Journal Pre-proof

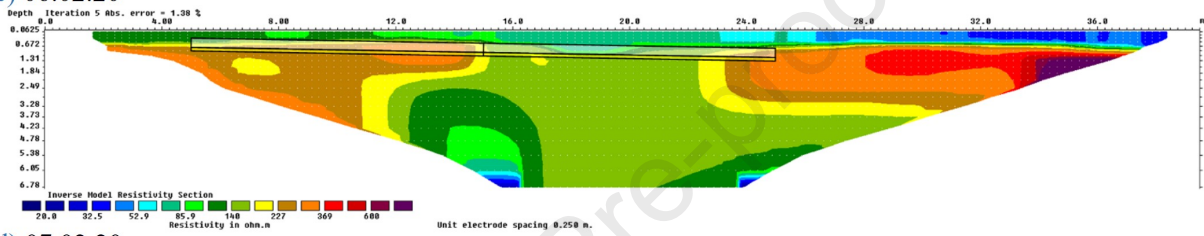
(a) 14.05.19



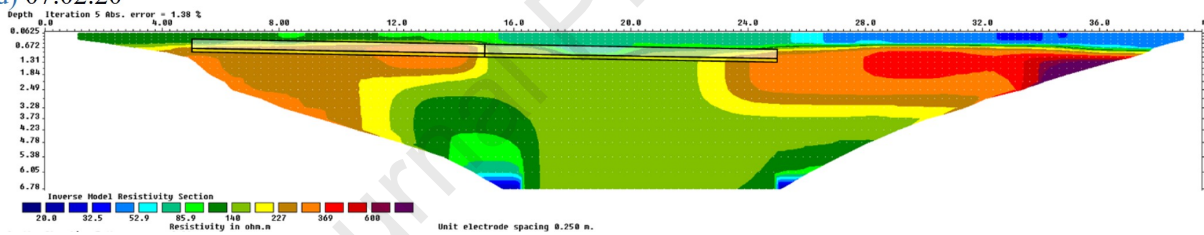
(b) 15.05.19



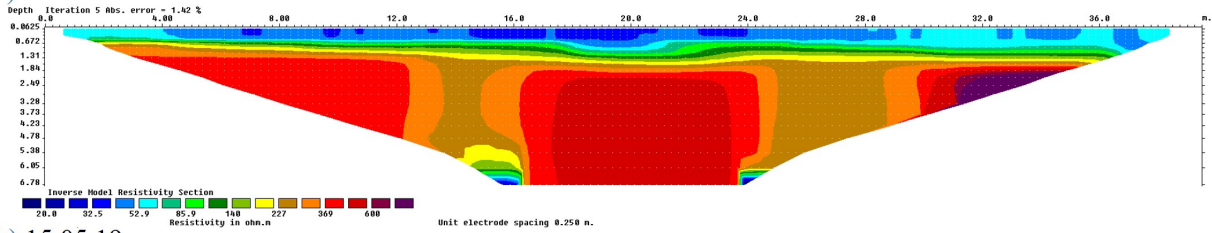
(c) 06.02.20



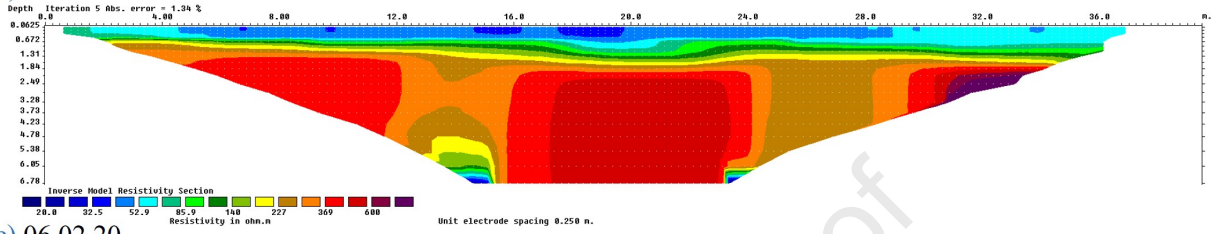
(d) 07.02.20



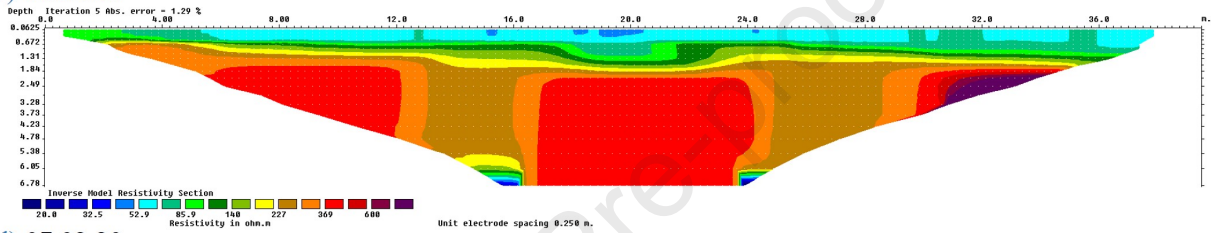
(a) 14.05.19



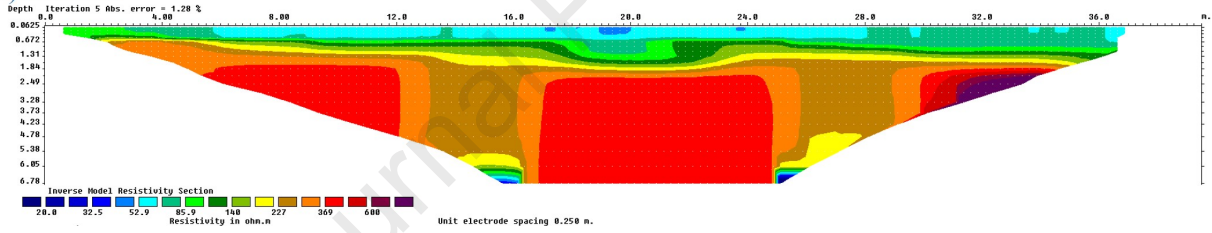
(b) 15.05.19

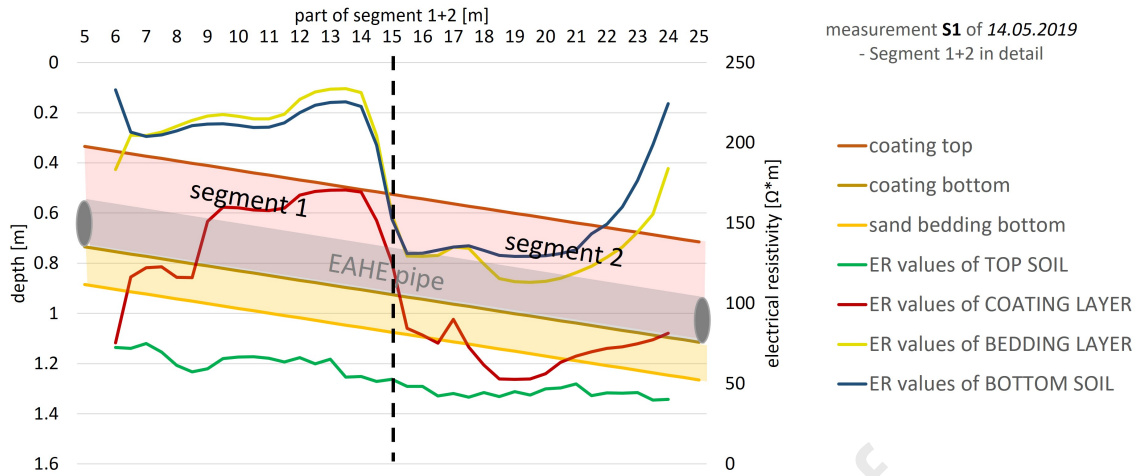


(c) 06.02.20



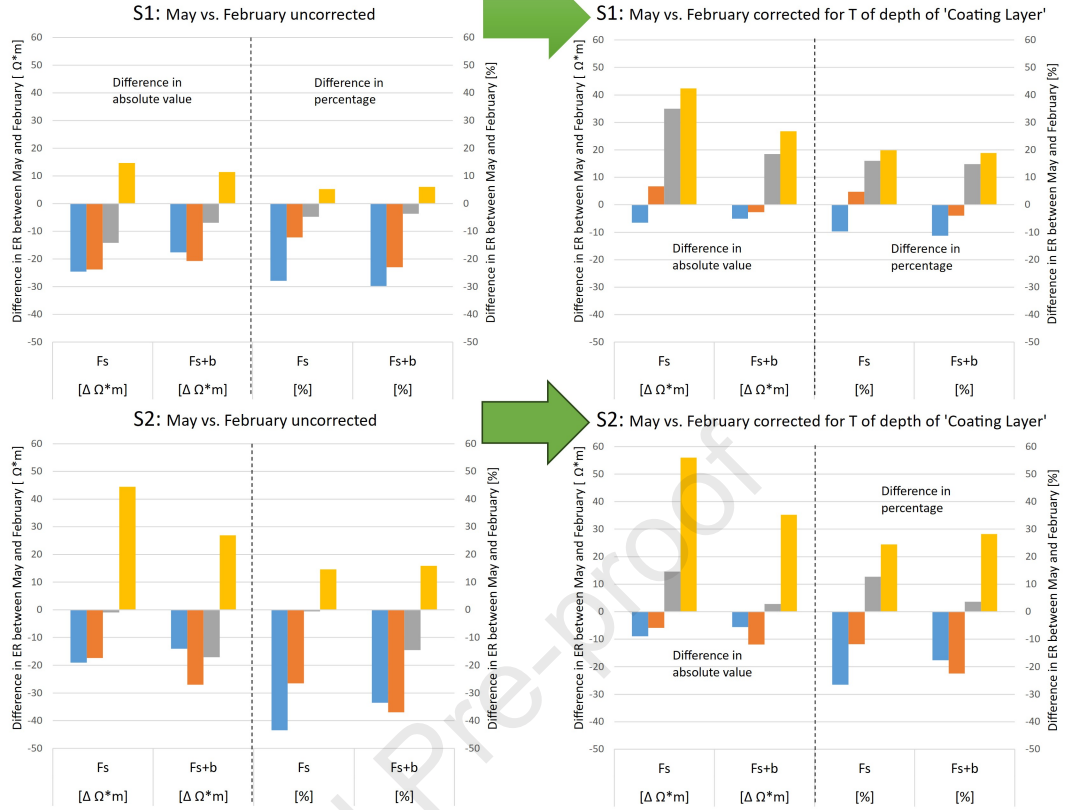
(d) 07.02.20

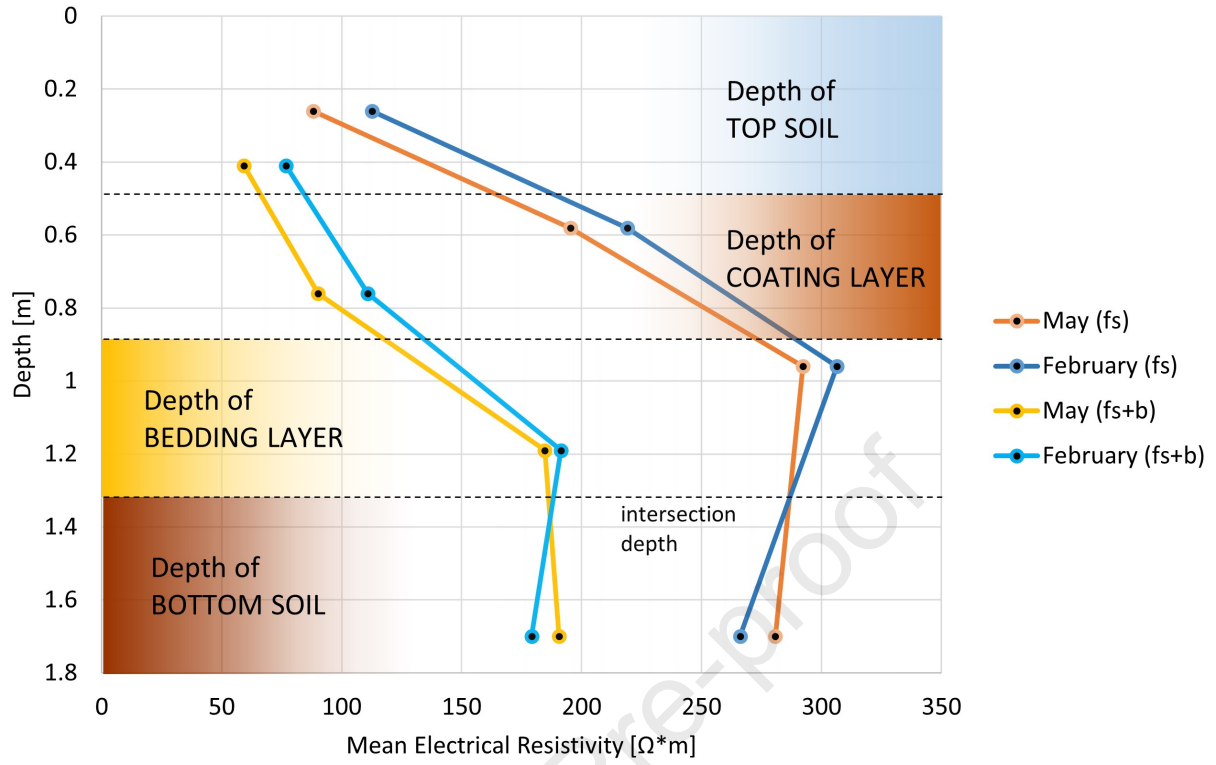


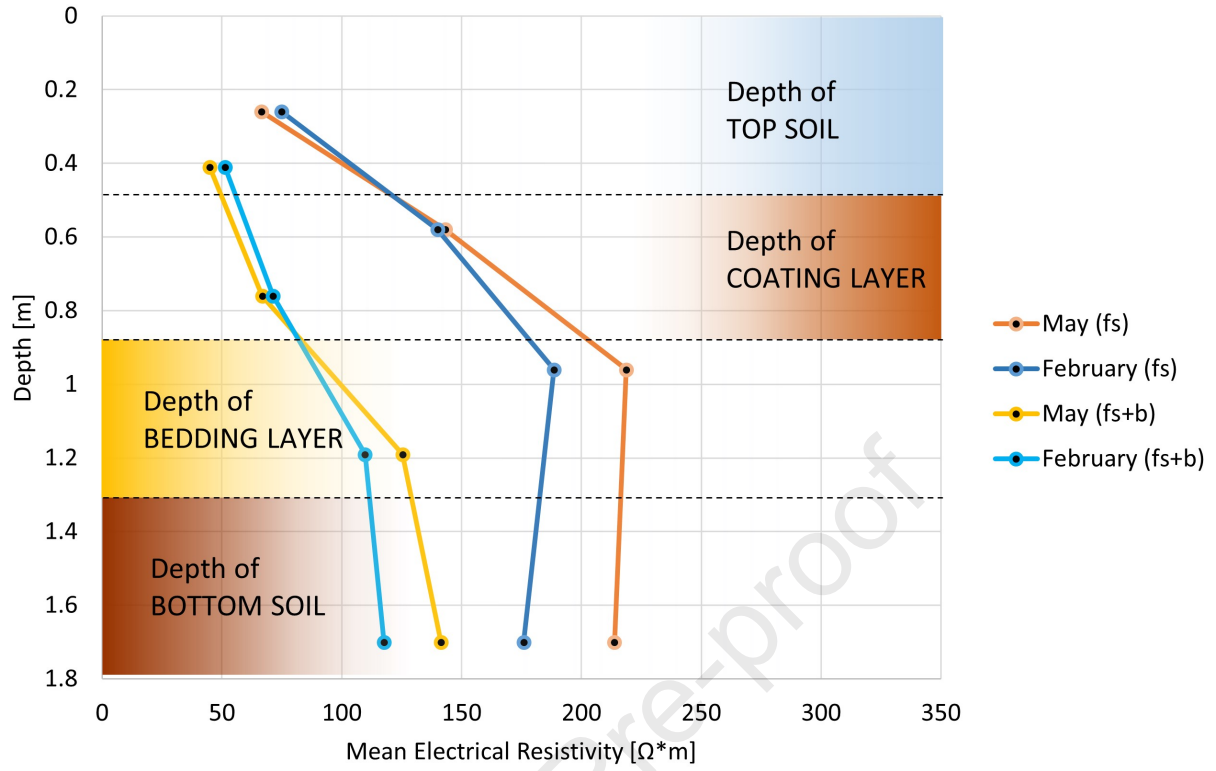


Journal Pre-proof

- Topsoil
- Coating Layer
- Bedding Layer
- Bottom Soil







Declaration of interests

- The authors declare that they have no known competing financial interests or personal relationships that could have appeared to influence the work reported in this paper.
- The authors declare the following financial interests/personal relationships which may be considered as potential competing interests:

Casey Canfield reports financial support was provided by Alfred P Sloan Foundation. co-author serves in uncompensated advisory role for the Green-e Governance Board - J. H.

Journal Pre-proof